PERFORMANCE EVALUATION OF (HVOF) THERMAL SPRAY COATING USING INCONEL-625 POWDER

BY

Hussain Yahya Al-Fadhli

A Thesis Presented to the

DEANSHIP OF GRADUATE STUDIES

KING FAHD UNIVERSITY OF PETROLEUM & MINIRALS

DHAHRAN, SAUDI ARABIA

In Partial Fulfillment of the
Requirements for the Degree of

MASTER OF SCIENCE

In

MECHANICAL ENGINEERING

June 2003

ACKNOWLEDGMENTS

First of all I thank ALLAH, who bestowed me with the strength to complete this work.

I shall always remain indebted to my thesis advisor, Dr.Zuhair Mattoug Gasem, who helped me throughout my thesis by his invaluable inspiration, encouragement and continuous guidance. He was always there to help me in the difficult times during the thesis. I am also extremely thankful to Dr. Bekir Sami Yilbas for his valuable suggestions and guidance in developing my background in the thesis subject. I am deeply gratefull to Dr. Khaled Mazghani, Dr. Amro Al-Qutub and Dr. Ibrahim Allam for their help, support and enhancement of this work.

I am grateful for the support of the Mechanical Services Shops Department, Martial Testing and Metallographic Group/ CSD, Corrosion Testing Unit/R&DC at Saudi Aramco and Mechanical Engineering Department at King Fahd University of Petroleum and Minerals for supporting this research work. This research would not have occurred without utilizing their laboratory facilities, their support is acknowledged.

I am extremely thankful to my colleague Mr. Mohammad Abdullah Al-Sultan, who helped me through out this work. His cooperation is acknowledged.

Finally, I would like to thank my parents and my wife who prayed and provided me the moral support that I needed the most throughout my Master Degree Study.

TABLE OF CONTENTS

LIST OF FIGURES

LIST OF TABLES

ABSTRACT

FULL NAME OF STUDENT: HUSSAIN YAHYA AL-FADHLI
TITLE OF STUDY: PERFORMANCE EVALUATION OF (HVOF) THERMAL SPRAY COATING USING INCONEL-625 POWDER

MAJOR FIELD: MECHANICAL ENGINEERING
DATE OF DEGREE: June 2003

A variety of metallic and ceramic coatings are available to protect metallic surfaces from high temperature, wear, and corrosive environments. These coatings are applied by one of many commercially available thermal spray techniques. In Saudi ARAMCO, high velocity oxygen fuel (HVOF) spraying technique is widely used to enhance erosion and corrosion resistance of steel surfaces and frequently used to repair worn away parts and equipments; which will improve availability and reduce operational cost. There are several setting parameters that can be adjusted by the applicator which can affect the performance of the applied coatings among which the powder feed rate and the spray distance are of prime importance. The aim of the present study is to examine the influence of varying powder feed rates and spray distances on nickel-based alloy powder coatings (Diamalloy-1005) applied on steel substrates using HVOF.

Four different coatings were produced employing low (5 lb/hr) and high (20 lb/hr) feed rates each sprayed at a spray distance of 9 and 12 inches. A variety of tests were employed to evaluate the performance of the different coating conditions. Microstructural investigation involved estimating oxide and porosity contents. Mechanical properties of the coatings were characterized by microhardness and tensile bonding strength tests. Accelerated corrosion tests and mass loss due to jet impingements tests were carried out to characterize corrosion and erosion resistance.

Experimental results suggest that for a given spray distance, the higher powder feed rate was associated with increased porosity contents and lower coating hardness. Coats produced at longer spray distance for a given feed rate exhibited higher oxidation content and lower hardness. Higher corrosion rates and higher mass losses were characteristics of coats produced at the higher feed rate with increased susceptibility at the higher spray distance. Limited bonding strength tests showed that HVOF coatings applied with higher feed rate exhibited lower bonding strength. Coatings applied with lower feed rate showed bonding strength more than 10,000 Psi.

ملخص الرسالة

الاســــــــــــم : حسين يحى عيسى الفاضلي

عـنوان الرسالـة : تقييم كفاءة التغليف المعدني ذو السرعة العالية باستخدام مادة (انكونيل652)

الــتــخــصــص : هندسة ميكانيكية

تـاريـخ الـتـخـرج : : يونيو/ 2003م

يجب أخذ التغليف المعدني ذو السرعة العالية بعين الاعتبار لحماية الاسطح المعدنية من درجات الحرارة العالية والتآكل البيئي إلا أن حماية الأسطح المعدنية ليست السبب الوحيد لاستخدام هذا النوع من التغليف بل الهدف الأساسي هو إطالة عمر هذه الأسطح مما يلعب دورًا أساسيًا في إبقاء مكائن الإنتاج الصناعي عاملة بفعالية أكبر,عوضًا عن تقليل تكلفة الصيانة الدورية.

والجدير بالذكر أن هناك عوامل أخرى ذات تأثير رئيسي على خصائص هذا النوع من التغليف وخاصةً الجزيئات الغير مذابة ونسبة الأكسسجين الموجودة في التغليف. ومن أهم هذه العوامل :كمية البودرة المذابة من مادة (انكونيل 625) ومسافةالضخ.

ولقد كان الغرض من هذه الرسالة هو دراسة مدى تأثير و فاعلية هذين العاملين على خصائص التغليف المعدني المكون من مادة (انكونيل 625) ؛ علمًا بأن هذه العوامل لها تأثير جذري على مسامية التغليف ومدى تحمله لمواجهة التآكل. وهناك تجارب عديدة عملت لتحديد جودة هذا النوع من التغليف مثل ؛ البحث في خصائص جزيئات المواد ,قياس نسبة الأكسجين فيها وقياس مدى صلابتها . إضافةً إلى ذلك ,فقد أجريت اختبارات على مدى تآكل هذا النوع من التغليف ومدى تحمله لقوة ضغط السوائل الحاملة لجزئيات الرمل كمياه البحر. وعلى هذا يتم تحديد مدى تحمل هذه المادة للظروف البيئية في منطقة الخليج العربي.

لقد اتضح من خلال هذه الدراسة أنه كلما ازدادت كمية بودرة (انكونيل 625) المدفوعة إلى جهاز التغليف كلما ازدادت مسامية المنتج و نقصت صلابته ؛ كما أنه كلما ازدادت مسافة الضخ كلما أعطيت جزيئات التغليف مجالاً أكبر لتفقد طاقتها الحركية, مما يجعلها تتأكسد وبالتالي تكون أكثر عرضة للتآكل بشكل كبير.

Chapter 1

INTRODUCTION AND BACKGROUND

1.1 INTRODUCTION

In the oil and gas industries, wear and corrosion of the internal parts of rotating and stationary equipment have direct effects on equipment durability and reliability. Thermal spray coating is a technology that has provided a significant improvement to the material surface properties. Material properties like wear and corrosion resistance play major roles in the surface behavior [17].

Materials, either in powder or wire forms, are melted and propelled to metallic substrate surface to form a coating. Regardless of the type of spray equipment and coating material (wire or powder), thermal spraying is involved with projection of molten or semi-molten particles against the substrate material. As the particles impact the surface, they are flattened and form thin splats or lamellae (Figure1.1). The splats bind to the substrate and to each other. The flattened particles build up and form the coating. Thermal spray systems typically consist of a gun, which uses combustible gases or an electric arc; gas control console or power supply; and a powder or wire feeder [2].

The High Velocity Oxygen Fuel (HVOF) thermal spray process has been basically developed to produce extremely high spray velocity. The system consists of six major components, including powder feeder, control unit, gas & fuel cylinders, spray gun, and air compressor. Fuel (Propane), air and gas (O_2) are adjusted in the control unit to produce the required combustion reaction with the specified temperature. Powder is injected into the system using nitrogen gas as a carrier, which is propelled at a high pressure to the surface (Figure 1.2). Combustion of the gases provides the exhaust velocity that plays a major factor in accelerating the particles sufficiently to achieve adequate bonding. The kinetic energy of the particles is so great, in fact, that most porosity, typical in a traditionally applied coating, is essentially reduced [4].

Low porosity and denser coatings are more wear resistant and can provide more protection per thousandth of an inch applied [1]. There are many parameters that need to be adjusted and optimized to achieve the best bonding with optimum coating quality. Among the key variables are surface preparation parameters such as grit type, blasting conditions, grit feed rate and sample surface roughness, or operational parameters like powder feed rate, stand off distance, gun pressure, work piece transfer speed and work piece surface temperature [26]. This work aims to investigate the effects of varying HVOF spray parameters on the structure of Inconel-625 coating (Ni 21.5-Cr 8.5-Mo 3-Fe 0.5-Co). Results can be utilized to optimize the coating performance according to the intended applications.

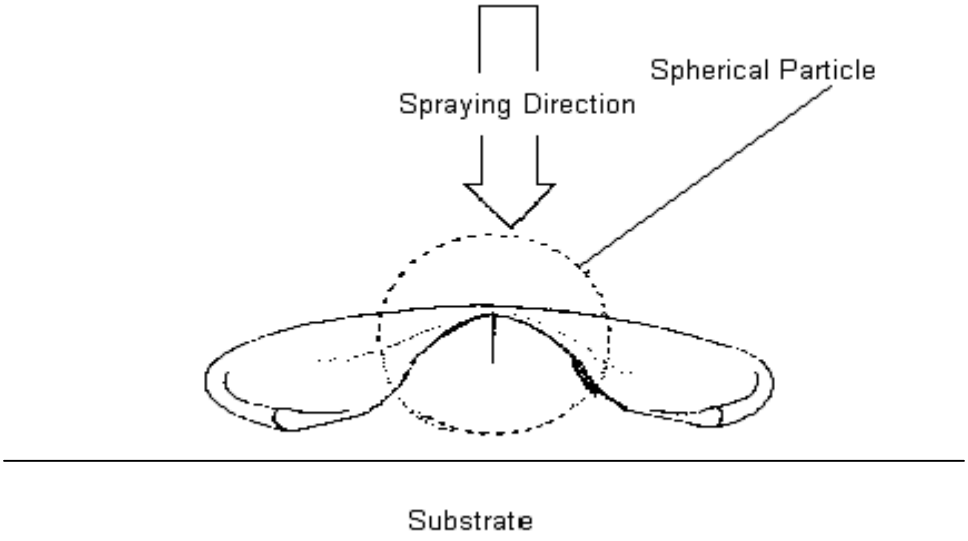

Figure1.1 Schematic diagram of thermally sprayed spherical particle impinged onto a flat substrate, [Pejryd, 1998].

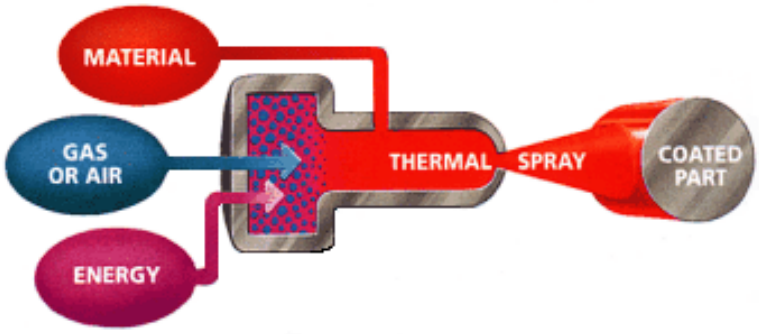

Figure1.2 Schematic diagram of HVOF spray system, [Sulzer Metco, 2002].

1.2 INTIATION OF THERMAL SPRAY COATING

Thermal spraying was first discovered and used in the beginning of last century and research in this field progressed ever since. The recognized beginning of Thermal Spraying is believed to be in 1911 in a flame spray process that was developed by Schoop from Switzerland. Other major thermal spray processes include wire spraying detonation gun deposition (invented by R.M. Poorman, H.P. Sargent, and H. Lamprey and patented in 1955), plasma spray (invented by R. M . Gage, O. H. Nestor, and D. M. Yenni and patented in 1962), and high velocity oxygen Fuel (invented by G. H. Smait, J. F. Pelton, and R.C. Eschenbach and patented in 1958), [32].

1.3 THERMAL SPRAY COATING TYPES

The group of thermal spray processes includes flame spraying, arc spraying, plasma spraying, detonation gun spraying, and (HVOF) spraying.

1.3.1 Flame Spray Process

Flame spray process uses combustible gas as a heat source to melt the coating material (Figure 1.3). This process is basically the spraying of molten material onto a surface to provide a coating. Coating material in both powder and wire form can be sprayed. The heat source is fuel gas–oxygen flame. Different fuel gases may be used including acetylene (C_2H_2) and propane (C_3H_8). The particle velocity is low (40 m/sec) because of the relatively low pressure and low flow rate [9].

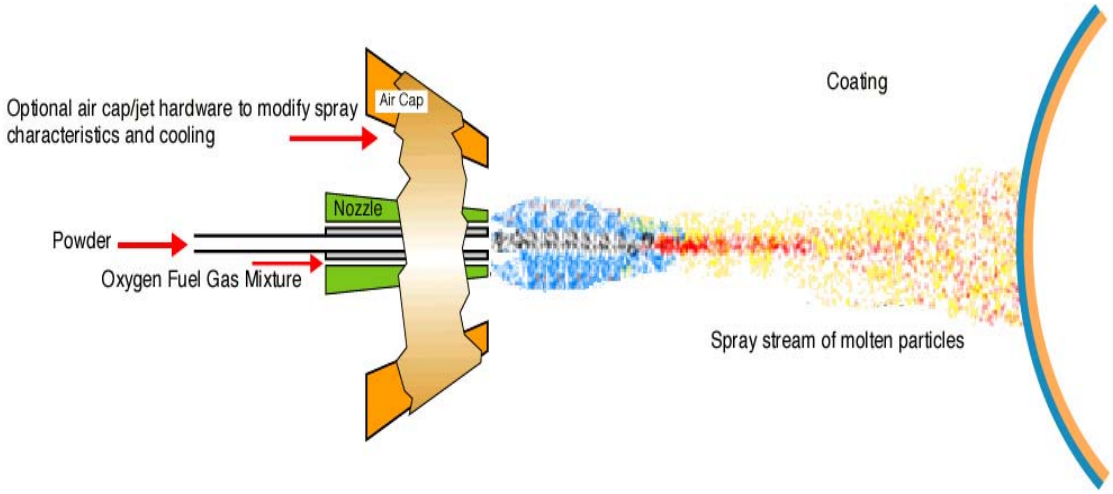

Figure 1.3 Schematic diagram of the flame spray process.

1.3.2 Arc Spraying Process

In the Arc Spray Process a pair of electrically conductive wires are melted by means of an electric arc (Figure 1.4). The molten material is atomized by compressed air and propelled towards the substrate surface. The impacting molten particles on the substrate rapidly solidify to form layers of coats. Electric arc spray coatings are normally denser and stronger than their equivalent combustion spray coatings. Low running costs, high spray rates and efficiency make it a good tool for spraying large areas and high production rates.

Disadvantages of the electric arc spray process are that only electrically conductive wires can be sprayed and if substrate preheating is required, a separate heating source is needed. The main applications of the arc spray process are anti-corrosion coatings of zinc and aluminum and machine element work on large components [2].

1.3.3 Detonation Gun Process

The Detonation gun basically consists of a long water cooled barrel with inlet valves for gases and powder (Figure 1.5). Oxygen and fuel (acetylene most commonly) is fed into the barrel along with a charge of powder [23]. A spark is used to ignite the gas mixture and the resulting detonation heats and accelerates the powder to supersonic velocity down the barrel. A pulse of nitrogen is used to purge the barrel after each detonation. This process is repeated many times a second. Operation frequency is typically four to eight cycles per second, giving a relatively low spray rate of 0.5 to 2 Ib/hr (0.3 to 0.9 Kg/hr) [3]. The high kinetic energy of the hot powder particles on impact with the substrate result in a build up of a very dense and strong coating [13].

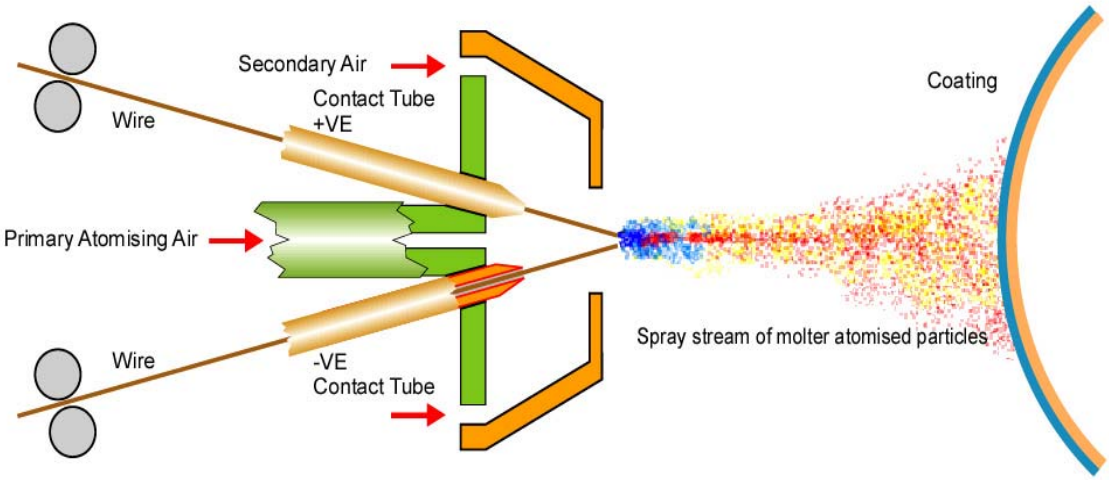

Figure 1.4 Schematic diagram of the electric arc spray.

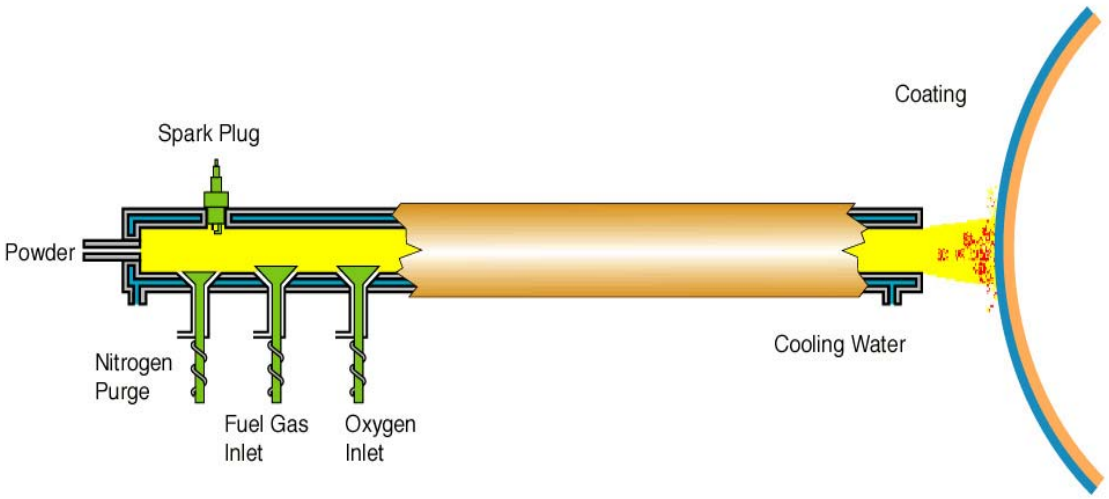

Figure 1.5 Schematic diagram of the detonation gun spray system.

1.3.4 Plasma Spray Process

The Plasma Spray Process is basically the spraying of molten or heat softened material onto a surface to provide a coating. Material in the form of powder is injected into a very high temperature plasma flame, where it is rapidly heated and accelerated to a high velocity (Figure 1.6). The temperature of the gas can be 15,000-20,000^{o}C, depending on the gas used. The hot material impacts on the substrate surface and rapidly cools forming a coating. Typical thickness applied by the plasma spray process is from 100 to 200 mills depending on the application and the type of material.

Plasma spraying has the advantage that it can spray very high melting point materials such as refractory metals like tungsten and ceramics like zirconia unlike combustion processes. Plasma sprayed coatings are generally much denser, stronger and cleaner than the other thermal spray processes with the exception of HVOF and detonation processes. Plasma spray coatings probably account for the widest range of thermal spray coatings and applications and makes this process the most versatile. Disadvantages of the plasma spray process are relative high cost and complexity of the process [32].

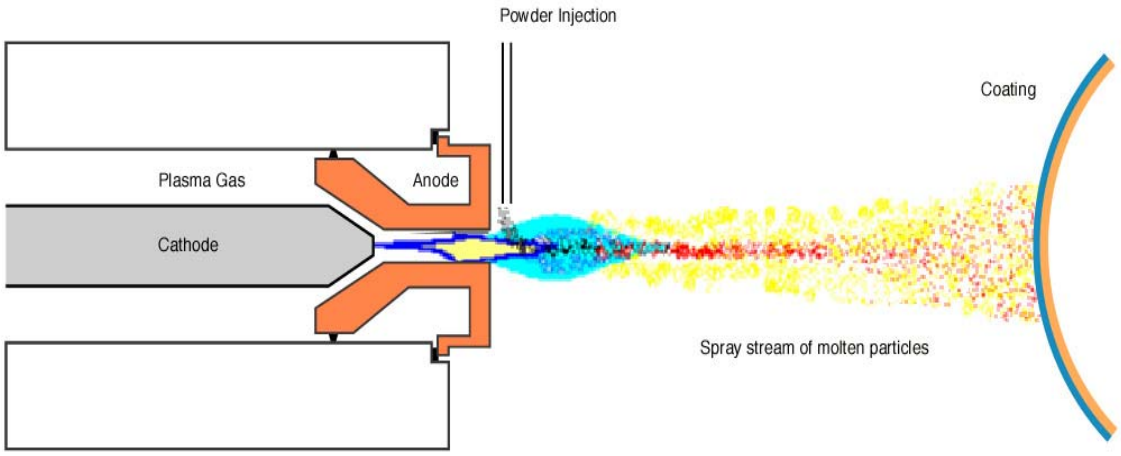

Figure 1.6 Schematic diagram of the plasma spray system.

1.3.5 High Velocity Oxygen Fuel (HVOF) Spraying

The High Velocity Oxygen Fuel (HVOF) Thermal Spray Process is basically the same as the powder flame spray process except that this process has been developed to produce extremely high spray velocity (Figure 1.7). This process is relatively new compared to other thermal spray Methods. Fuel (kerosene, acetylene, propylene and hydrogen) and oxygen are fed into the chamber, combustion produces a hot high pressure flame which is forced down a nozzle increasing its velocity. The coating material, which is a powder, is fed into the high energy gas stream where the expanding gas forces the particles through a nozzle at supersonic velocity. Gas velocity have been measured in the range from 1,500 to 2,000 m/s (4,900 to 6,500 ft/s), on the order of five times the speed of sound [23]. Flame temperature is relatively low, on the order of 2,900^{o}C (5,250^{o}F), making it difficult to spray ceramics and refractory metals. Since dwell time (time when the powder is in the flame) is short, heat transfer to large powder particles may not be sufficient. It requires finer powder particle size and tighter particle size distribution than other processes. The Ideal Stochiometric combustion equation for propane is:

$$C_3H_8 + 5O_2 \longrightarrow 3CO_2 + 4H_20 \qquad \Delta H = -2220KJ/mol\ C_3H_8$$

The compressed air pinches and accelerates the flame and acts as a coolant for the HVOF gun [13]. The coatings produced by HVOF are similar to those produce by the detonation process. HVOF coatings are very dense, strong and show low residual tensile stress or in some cases compressive stress, which enable thicker coatings to be applied than previously possible with the other processes [13]. The very high kinetic energy of particles striking the substrate surface does not require the particles to be fully molten to form high quality HVOF coatings. This is certainly an advantage for the carbide type coatings and is where this process really excels [12].

HVOF coatings are used in applications requiring the highest density and strength not found in most other thermal spray processes. New applications, previously not suitable for thermal spray coatings are becoming viable [6].

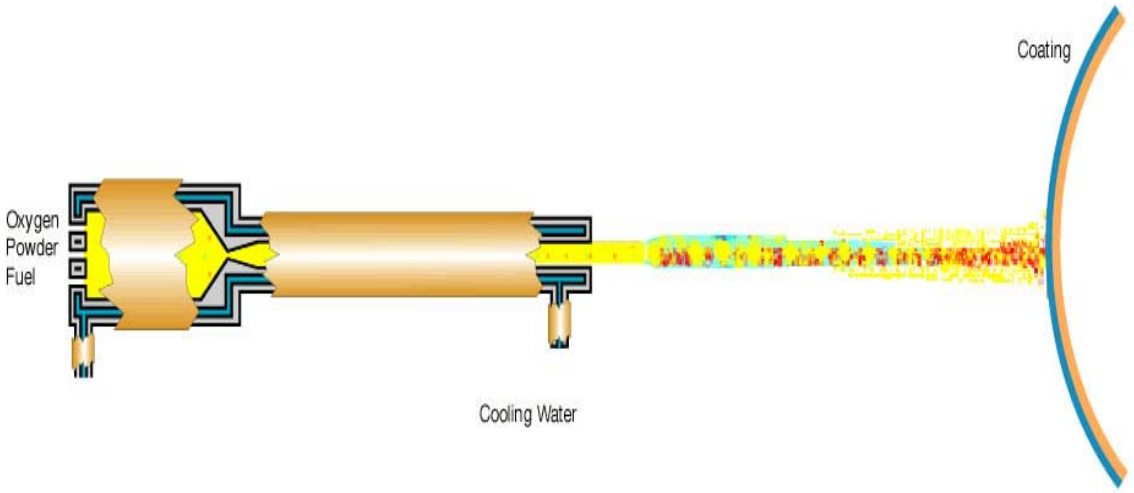

Figure 1.7 Schematic diagram of the HVOF spray system.

1.4 COMPARISON BETWEEN THERMAL SPRAY PROCESSES

The different thermal spray processes described have different characteristics. As shown in Table 1.1 the heating temperature and particle velocity affect the coating properties. Both spray distance and powder feed rate as a setting parameters produce different heating temperature and particle velocity. The HVOF- and D-Gun spray processes are characterized by higher particle velocities, consequently, the coated layers exhibit higher density and bond strength than coating produced by other processes [4].

Numerous feedstock materials are commercially available for powder spraying (Table 1.2). Nickel-based materials including Inconel-625 which is of our interest in this study, produce coatings that are generally hard and resistant to oxidation [17]. They may be used for mid-range to high-temperature service applications with some capable of service temperatures up to 1000°C (1850°F) [10]. Chemical compositions for these materials range from stainless steel type materials to super alloys, as well as NiCrAl and NiCoCrAl materials.

Table 1.1 Characteristic of thermal spray processes and coatings, [2].

Spray Process	Temperature (^{o}C)	Velocity (m/sec)	Adhesion (MPa)	Porosity (%)
Flame Spray (Powder)	3100	60-70	6-10	7-12
Flame Spraying (Wire)	3100	120-140	10-15	5
Arc Spraying	7000	100-170	10-20	3-15
Plasma Spraying	15000	150-600	20-70	1-8
Detonation Gun Spray	4200	600-800	60	<1
High Velocity Oxygen Fuel (HVOF)	2750	600-1200	>70	1-2

Table 1.2 Powder and wire feedstock materials [13].

Powder/Wire Types	Material Types					
Self-Fluxing Powders	Cobalt Base		Nickel Base			
Abradable Powders	Al Base	Cobalt Base	Copper Base		Nickel Base	
Ceramic Powders	Al Oxide	Chrome Oxide	Titanium Oxide		Zirconium Oxide	
Metal Alloy Powders	Al. Base	Co Base	Cu Base	Iron Base	Mo Base	Ni Base
Carbide Powders	Chrome Carbide		Tungsten Carbide			
Arc Wires	Pure Metals	Al Base	Cu Base	Iron Base	Nickel Base	Tin Base
Combustion Wires	Pure metals	Al Base	Cu Base	Iron Base	Ni Base	Tin Base

1.5 HVOF COATING PROPERTIES AND APPLICATIONS

1.5.1 Restoration of Worn Machine Parts

The restoration of worn machine parts to their original dimensions and the build up of improperly designed or fabricated components were the earliest uses of thermal spray coatings. The reason why HVOF is preferred and used other than welding is due to the absence in distortion and heat affected zone, minimal residual stresses and less in oxidization. In the repair processes there are some characteristics need to be attained such as low shrinkage, ability to meet thick deposits, good adhesive and cohesive strength, finish characteristics compatible with the component, low cost feed stock and application hardware, and high deposition rate and efficiency.

1.5.2 Erosion-Corrosion Resistance

The adverse effect of fluids on a solid surface is the result of the complex interaction of chemical and physical forces. Direct exposure to liquids, gases, and particulate solids can quickly produce chemical corrosion or erosion of a solid surface. The high-speed movement of these corrosive fluids prevents the formation of protective oxides and permits this hostile interaction of corrosion or erosion to take place. Cavitation occurs when pressure changes in the liquid lead to the formation and collapse of vapor bubbles. This produces high-pressure shock waves that can destroy metallic surfaces. Particles within the fluid can impact the surface, damaging it even further [24]. HVOF with it's different powder characteristics could suit most applications to minimize the erosion or corrosion of the internal parts of the industrial equipments. The repair shops could customize it's requirements with the presence of the HVOF

coating. For instance, a carbon steel pump shaft could be coated with Inconel-625 to increase its corrosion resistance. The same shaft could be enhanced in terms of wear resistance if coated using Tungsten Carbides (WC) [2].

1.5.3 Wear Resistance

The single most common use for thermal spray technology is to retard and control wear. HVOF are used to enhance the hardness and finish characteristics of repaired surfaces, to minimize the effects of mechanical wear, and extend product life. In doing so, maintenance and operational costs are reduced and productivity and profits are increased. While there are several different wear phenomena that occur, such as abrasive wear, adhesive wear, fretting or sliding wear, they have a common result: surface material is lost, ultimately causing a functionally significant change in dimension and impaired performance. Mastering the wear process will directly affect the equipment reliability and durability.

1.6 PARAMETERS AFFECTING THE HVOF COATING CHARACTERIZATION

There are many parameters that have a direct effect on the HVOF coating characterization. These could be either surface preparation parameters such as grit type, blasting conditions, grit feed rate and sample surface roughness or operational parameters like powder feed rate, stand off distance, gun pressure, work piece transfer speed, work piece surface temperature and different equipments from different manufacturer produce different coatings structure [31].

1.6.1 Powder Feed Rate

The powder feed rate represents the amount of powder injected to the system. The powder feeder is the system that controls the flow of the powder utilizing the nitrogen gas as a carrier. The recommended powder feed rate by the HVOF equipment manufacturers (Sulzermetco) for the Inconel-625 is in the range 5 to 20 Ib/hr. If the amount of powder is very high the probability of having non-melted particles in the surface is high [26].

1.6.2 Spray Distance

The spray distance is how far the spray gun is from the work piece. The recommended spray distance by the HVOF equipment manufacturer (Sulzermetco) for the Inconel-625 is in the range of 9 to 12 Inches. If the spray distance is very small, the probability of having overheating in the substrate is high and if the spray distance is too big, the particles temperature will drop before it hits the surface. This drop in temperature will affect the coating bonding [19].

1.6.3 Scope of the Work

Since HVOF coating finds wide application in industry, investigation into influence of coating parameters on the resulting coating properties, such as bonding strength, miocrostructure including void formation, interface properties and wear resistance are essential.

In the present study, the influence of the stand-off distance (distance between the gun nozzle exit and workpiece surface), powder feed rate on the microstructure, wear resistance, electrochemical response and the tensile bonding of the coating is investigated experimentally. To achieve the mentioned objective, an experiment is designed to include two levels of stand-off distance and two levels of powder feed rate. In order to secure standards, the work piece were prepared in accordance to Sulzermetco (HVOF equipment manufacturer) standards, and it was tested according to ASTM C 633 for tensile, ASTM G-5 for electrochemical test. The coatings of the workpiece were achieved at Mechanical Services Shops Department while microstructure analysis, jet impingement test and electrochemical test were conducted in the Research and Development Center R&DC in Saudi Aramco. The tensile bonding tests were carried out at the advanced material science lab of KFUPM.

Chapter 2

LITERATURE REVIEW

2.1 REVIEW OF PREVIOUS STUDIES

The following section is a brief review of the previous investigations carried out in this field with special attention being paid to the investigations carried out on HVOF coating parametric, microstructural, wear and corrosion experimental studies.

Berget, J., [2] Carried out an experimental analysis on the influence of different HVOF spray parameters and powder characteristics (WC-Co-Cr) on the structure, erosion and erosion-corrosion properties of the sprayed coating. Spray parameters investigated were: (i) the energy input, (ii) powder feed rate and (iii) the spray distance. All of these parameters were critical for the coating porosity and the fraction of retained tungsten carbide (WC). A high energy input increased decomposition of WC and thereby a reduction fraction of retained WC. The porosity at high energy input was low. An increase in the powder feed rate increased both the fraction of retained WC and the porosity. A long spray distance (12-15 inches) may have also increased WC decomposition. Powder characteristics studied include: (i) average WC particle size (ii) relative amount of Co and Cr in the metallic binder phase and (iii) powder grain size distribution. The powder and coating were characterized by different methods including Scanning Electron Microscope (SEM), Optical Microscope and X-ray diffraction (XRD). Erosion and erosion-

corrosion properties of the coatings were investigated by specially developed equipment. Smaller WC particles were superior from the point of view of erosion and erosion corrosion performance. An increase in Cr content increased the erosion-corrosion resistance at low erosive conditions. Powder with narrow grain size distribution resulted in coating with higher quality than corresponding powder with wider grain size distribution.

Hackette, C., [8] Carried out an experimental study of the influence of the gas dynamics on the HVOF particles properties and results showed the effect of these properties on the coating integrity. Within this experimental process a hot combustion driven, supersonic jet was used to propel particles onto a surface, thus forming metal coating that provides wear, temperature, and corrosion resistance. The author studied the fundamental physics of the spray process and confirmed this study with several experiments. A simple numerical model was developed to predict the behavior of the spray particles in the HVOF jet. The results of computation indicated that independent control of spray particle velocity and temperature was possible through schematic variation in combustion chamber pressure and particle injection location within the nozzle. This hypothesis was confirmed through a series of experiments in which stainless steel particle velocity and temperature were measured using trace velocimeter and two color radiative pyrometer, respectively. Combustion chamber pressure had strong effect on particle velocity. Injection location was used to control the residence time of a particle within the flow, thus allowing manipulation of particle temperature without a measurable effect on velocity. The results of these experiments revealed that the behavior of the compressible gas flow of the HVOF spray process strongly influenced spray particle properties, which, in turn, affect coating properties.

Shimizu, Y., et al., [27] carried out an experimental study on the enhancement of the HVOF coating deposition efficiency and hardness. Three different guns of varied geometry were designed and tested experimentally. The spraying process was simulated numerically for each of the nozzle geometries to understand their effectiveness in influencing the velocity and temperature of the sprayed particles. The coating was characterized using optical and scanning electro microscope (SEM) , Micro-Vicker hardness test and X-Ray Difractometry (XRD). Result showed that with the use of convergent and divergent gun type nozzle , the extent of the melting of the alumina particles will be increased. This was exhibited by an increase in the deposition efficiency (amount of material adhered to amount of material sprayed) to the extent of 45%. However, the sharp change in the convergent and divergent nozzle geometry, result in fusion and agglomeration of alumina particles leading to the spitting during the spraying process. The result showed that alumina coating of excellent hardness 920-1290 HV, with a relatively dense microstructure could be obtained in HVOF method irrespective of the gun nozzle geometry, providing the spraying parameters are properly controlled.

Skandan, G., [28] studied the wear properties of HVOF sprayed hard coatings produced from different powders feed stock materials. The different materials were WC/Co conventional powder produced from Metco with size 2-5 micro meter and the second material were WC/Co nano particles produced from Nanodyne powder Co. with size 0.03 micro meter in diameter. The third material which is the one of interest is a combination of the two materials produced by blending the conventional powder with the nano-phase powder (Multimodal), followed by heat treatment to bond the agglomerated particles together. For each powder, a sliding wear test were conducted using ball and disk tribometer at sliding speed of 18-30 mm/s, load 9.8 N and sliding distance from 24-12000 m. Wear volume of both WC/Co disk and Si_3N_4 ball were determined and showed that multimodal powder offers about 50% improvement in abrasive and sliding wear

properties relative to the other materials. Amount of decarburization were decreased from 83% in Nanograined WC/Co to 10% in conventional powder and to 1.7% in multimodal powder.

Krepski, R., [13] studied the erosive wear, cavitation erosion on the HVOF and plasma spray caused by turbulent flow of pumps and turbines. This flow can induce local pressure drops below the vapor pressure of the liquid, nucleating gas bubbles. The shock waves from the collapse of these bubbles causes the surface damage. The author studied several thermal spray coatings that might suit applications such as metallic materials, ceramics and carbides. Results of the studies reveal that the main problem of metallic coating is the presence of oxide films between splats, which provide preferred path for crack propagation. Spray and fuse chromium was found to be the best of metallic materials tested. Aluminum oxide which has high inherent strength and alumina-zirconia which has a dispersion of submicron zirconium oxide are good performers. For this application, the fact that ceramic splats are incompletely bonded to each other may be an advantage that allow some elastic response under the oscillating stress field.

Legoux, J.G., et al., [14] made an experimental study on four different High Velocity Thermal Spray Guns using one powder WC-10Co-4Cr. A parametric study was carried out for each type. These parameters are Nozzle size, gas rate, and powder feed rate. The results were compared in terms of deposition efficiency, substrate temperature, particle velocity, particle temperature, porosity, hardness and volume loss. Spray conditions were ranked according to porosity, hardness and deposition efficiency.

Gourlaouen, G., [7] made an experimental study on a stainless steel sample to show the effect of spray parameters on the coating properties. HVOF spraying process is widely used to improve components life in service. However, many parameters can affect metallic coating properties, especially unmelted particles and oxidation level. Flame parameters such as combustion ratio and temperature, are of prime importance. The aim of their work was focused

on the influence of those parameters on stainless steel coating as a substrate. The conclusion of this study showed that the influence of the combustion temperature was small. On the contrary, an increase of the flame power led to higher oxidation with low unmelted particles rates and the deposition efficiency was improved. Among the three parameters studied, the combustion ratio had significant influence. Its increase, in the domain considered, was involved with a decrease of the oxygen content, and consequently of the micro hardness, but an increase of the number of unmelted particles resulted in a decrease of the deposition efficiency.

Brandt, O., [5] studied the wear resistance of different carbide coatings using standard abrasive wear testing methods. Two commercial HVOF flame spray processes were used to apply various tungsten carbide coatings. Process parameters influencing the coating properties were compared with regard to wear resistance. Standard tests used were (ASTM G 65-85). The total wear length was 80m (divided into four steps) using a steel wheel instead of a rubber wheel. The weight loss was measured on a laboratory scale of 0.0001 gm. The wear test carried out at room temperature without cooling. The test specimen was constructed of Steel ST 37–II (I = 60mm, w = 35mm, t = 10mm) with a 0.5 mm coating of HVOF WC 17% Cr. Results showed that wear resistance of the coating increased with increased fuel/oxygen flow ratio, and this is mainly due to the enhancement gained in the energy input. The best wear resistance and the highest hardness were reached with specific flame condition (fuel/oxygen flow ratio of 0.2). An oxidizing flame condition (fuel/oxygen flow ratio <0.6) yielded a lower hardness of the coating with corresponding decrease in wear resistance. Reducing the spray distance from the base line condition 250 mm (9.8 Inches) led to an increase in the hardness and wear resistance. Increasing the spray distance increased the hardness of the coating as well, but its wear resistance decreased.

Suman, S., [30] studied the morphology, composition and erosion-cor-rosion behavior of Ni-Cr-Si-B cermet coating overlaid on a carbon steel substrate by high-velocity oxygen-fuel (HVOF) thermal spraying. He studied the coating in three different conditions as sprayed followed by a resin impregnation process carried out under vacuum and as sprayed followed by a high temperature vacuum fusion operation. His experimental work involved using an impinging jet facility with suitable electrochemical monitoring. The electrochemical experimental results were supported by post test microscopical analysis using light microscopy, scanning-electron microscopy (SEM), energy dispersive spectroscopy (EDS), X-ray diffraction (XRD) and atomic force microscopy (AFM) to characterize changes in the microstructure of the coatings after erosion-corrosion. The microscopy of as sprayed and vacuum sealed coatings showed almost similar microstructures typical for thermal sprayed coatings with good adherence and low porosity, however after vacuum fusion, the microstructure changed significantly forming a basal with characteristics different from the bulk coating away from the interface. Erosion-corrosion tests were carried out in a solid-free sea-water impinging jet of velocities 17, 25, 50 and 72 m/s at temperatures of 180^{o}C and 500^{o}C. The behavior of the coatings was followed by undertaking electrochemical (E/C) monitoring during the impingement corrosion process. This involved anodic polarization scans which have demonstrated the effect of the impinging jet and increased temperature in reducing the resistance of the coating under erosion-corrosion conditions in comparison with corrosion in static sea-water and corrosion at ambient temperature.

Chapter 3

EXPERIMENTAL SET-UP

3.1 HVOF SPRAYING EQUIPMENT

A Sulzer Metco Manual Hybrid Diamond Jet (using propane fuel gas) with DJ9H - Hand held gun body, 9MP-DJ powder feed rate control, and DJFW precession flow meter were used to produce the coating (Figure 3.1(a)). Air, fuel and oxygen were maintained at pressures 105, 90 and 150 psi, respectively. The work specimen was maintained at 300 ^{O}F and rotating at 250 rev/min using a Dean Smith B-5 lathe machine (Figure 3.2).

3.1.1 Spraying Gun

The Sulzermetco HVOF spraying process uses oxygen and fuel gas to produce a high velocity gas stream in the gun nozzle. This gas stream, when ignited as it exits the gun, becomes luminous white, supersonic flames that contains diamond-shape shock waves (hence the name "Diamond Jet") (Figure 3.1(b)). The combination of high fuel gas and oxygen flow rates and high pressure lead to the generation of supersonic flame. The gun could accommodate different fuel gases including acetylene (C_2H_2), ethylene (C_2H_2), propylene (C_3H_6), propane (C_3H_8) and Hydrogen (H_2). The coating material, which is powder, is fed into the high energy gas stream where the expansion gas forces the particles through the nozzle at supersonic velocity. The high kinetic energy of the powder gives well bonded coatings with high bond strength and low porosity [2]. HVOF systems from different manufactures may be quite different. Dave Harvey et al [9] describe different HVOF systems and important differences between them. Significant details making them quite different from each other are powder feed position in the spraying gun and gas flow rates. In some systems the powder is fed in the combustion, in other systems is fed in the exhaust barrel. Feeding powder in the combustion chamber, like the gun we are using' maximize the heat transfer to the powder particles. This increase in the heat transfer, in parallel with the spray distance and the powder feed rate variable variation plays a major roll in coating oxidation. Hybrid cooled spraying gun specifications are available in Appendix A.

Figure 3.1(a) High velocity oxygen fuel system (Sulzermetco, 2002).

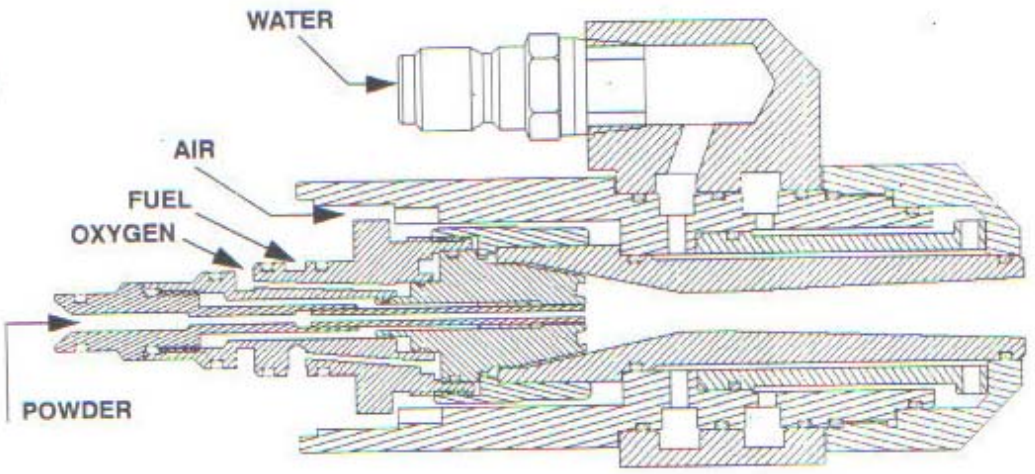

Figure 3.1 (b) Schematic diagram of DJ HVOF spraying gun (Sulzermetco, 2002).

3.2 POWDER MATERIAL

Nickel base alloy (Diamalloy 1005) manufactured by Sulzermetco company with 45 ± 11 μm size was used. These particles had spherical shape and are similar to Inconel-625 properties and composition (Table 3.1). It is used in corrosive and erosive applications like seawater environments.

Table 3.1. Chemical Composition of Diamalloy 1005 Powder.

Powder Material	**Chemical Composition**				
	Ni	Cr	Mo	Fe	Co
Inconel-625	66.5	21.5	8.5	3	0.5

Figure 3.2 Photograph of the HVOF system and the work piece during spraying.

3.3 WORKPIECE

The work piece material was Carbon Steel AISI 4140 of cylindrical shape and had the following dimensions: Diameter (D) = 1 inch and Length (L) = 6 inches. Microstructure investigations were made on a cross section of the work piece (Figure 3.3). Workpieces were fabricated at Saudi Aramco, Mechanical Services Shops Department (MSSD).

3.3.1 Sample Preparation

One of the major problems is how to relate the sample spraying to the actual work, which is difficult since the samples are very small in comparison to the actual parts. According to MSSD capabilities, the samples were spayed in special mechanism that is closely related to the actual work (Figure 3.4). The limitation of the system was that the samples have to be sprayed while it is rotated. The mechanism will make varying the spray distance more easy, in which we could spray more than one sample with different spray distance at one setup. Since the objective was to coat the samples tip, an epoxy was added to the cylinder surface. This epoxy prevented the bonding in between the coating and the cylinder outer surface. Another advantage of having this setup is to allow making the adhesion test according to ASTM C 633.

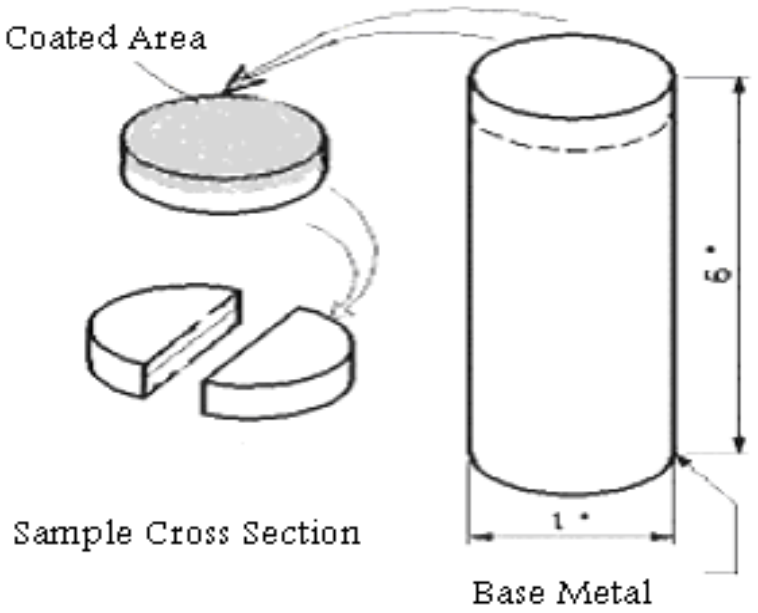

Figure3.3 Schematic diagram of the coated sample.

Figure 3.4 Photograph of samples mechanism.

3.3.2 Surface Preparation

Since the quality assessment is part of this study objective, proper attention has been paid to the condition of the substrate surface prior to spraying. Samples were cleaned using a steam cleaning process. The main advantage of the cleaning is to remove any contamination at the surface. To ensure the removal of the hydrocarbon on the surface, the samples were sent to the oven for preheating. Preheating temperature was $300^{O}F$ and the duration was two hours. The samples were grit blasted using (Al_2O_3) grit blasting sprayed at pressure of 80 psi (Figure 3.5). Roughness was characterized by a profilometer, which yields an arithmetic average of peak and valley positions relative to the mean surface plane. The profilometer reading was from 20 to 30 μm. After finishing the grit blasting the samples were sent immediately for spraying before it suffers from moisture contamination.

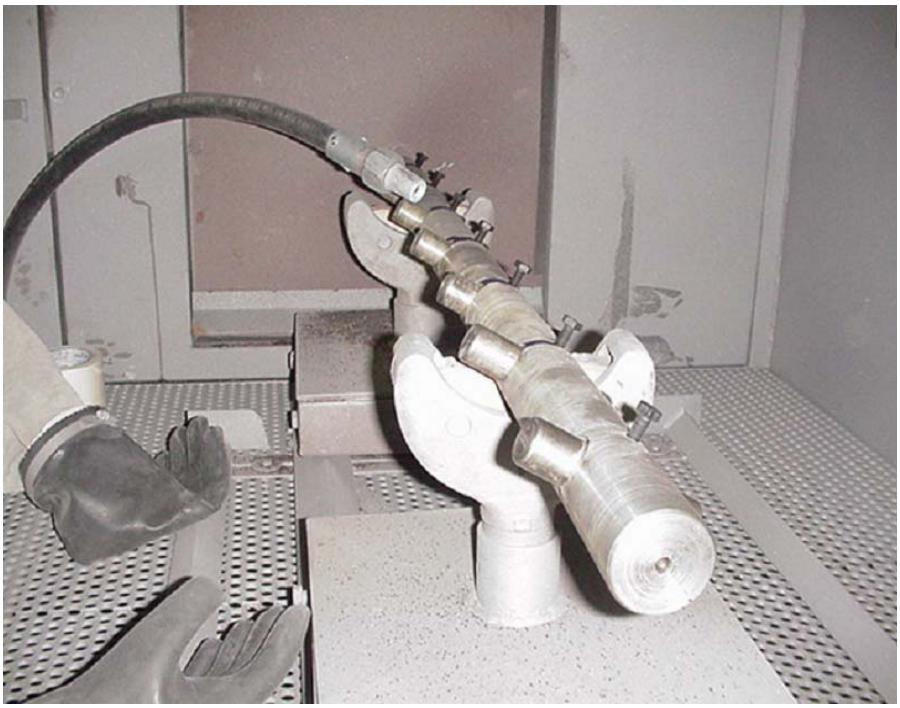

Figure 3.5 Photograph of grit blasting chamber.

3.4 HVOF PROCESS PARAMETERS VARIATION

3.4.1 Powder Feed Rate

The powder feed rates were varied from 5 lb/hr to 20 lb/hr (Table 3.2). These two variations represent the lowest and the highest rate recommended by the equipment manufacturer. Wide variation was chosen to see the real effect of the powder feed on the coating integrity. The literature pointed out that if the powder feed rate increases at constant energy input, the same amount of energy can be used to melt a high amount of powder, but particle temperature will decrease. The reduction in the particle temperature will result in a more porous coating. Coating build up rate also can be affected by the powder feed rate. When the build up rate is high, the probability of having cracks within the surface region will increase.

Table 3.2 Spray parameters for the coated samples.

Coating	Number of Samples Fabricated	Powder Feed Lb/hr	Spray Distance Inches
1	3	5	9
2	3	5	12
3	3	20	9
4	3	20	12

3.4.2 Spray Distance

Spray distance control is an important factor that affects the coating structure. In this experiment, the lowest (9 inch) and highest (12 inch) recommended by the equipment manufacturer were applied (Table 3.2). Many factors can be affected by the spray distance variation such as coating oxidization, porosity, particle temperature at impact, loss of kinetic energy and coating build up rate. Possibility of having more oxidization is increased when the spray distance is lengthened. At longer spray distance, the particles temperature will decrease and the coating will be more porous. Conversely, the substrate will be over heated and the percentage of unmelted particles will increase when the spray distance is short. Different powders with different spraying parameters are available in Appendix A.

3.5 COATING CHARACTERIZATION

3.5.1 Microstructure Analysis

SEM (Philips XL-30) equipped with energy dispersive spectrometer (EDS), Model DX-4 by EDAX (Figure 3.6) and optical microscopy (REICHERT MEF4 A) were used to characterize the structure and the porosity of the coating. Samples were cut in half using a diamond cutoff wheel. The samples were ground and polished using ECOMET3 disc at rotational speed of 120 rpm using water as a lubricant. The equipment used was manufactured by Bulhler. The time at each step was three to four minutes. Each coating condition had two identical samples for each microstructural analysis. The characterization was done for each case separately. Porosity was quantified using the image analysis software integrated with the electron microscope. This occurred through capturing the digital image of the coated sample using the backscattered electron detector and optimizing the gray levels of the sample surface defects such as porosity.

3.5.2 Microhardness Test Preparation

Microhardness was measured using a Leica Vm Htmot hardness tester that has a test load of 500 g according to ASTM E-384. The microhardness test was considered for each coating set. For instance, variation of hardness with spray distance, variation of hardness with powder feed rate and variation of hardness with coating thickness for each case. The hardness tests were taken in the coated area of the prepared sample. Nine vertical and horizontal readings were taken for each sample with optical microscope observation. The specimens were metallographically polished. The indenter is a pyramidal of normal dimensions and could be charged with a load of 0.1 N to 50 N. As per literature review, measurements under low load such as (0.5N) describe the micohardness under different lammela and measurements under high load such as (10, 15 N) describe the microharness of the whole coating [13].

Figure 3.6 Photograph of ESEM (Philips XL-30).

3.6 ELECTROCHEMICAL TEST PREPARATION

The procedure for corrosion rate determination in the simulated solution by the electrochemical technique as per ASTM–G 5 can be summarized as:

- Preparing the electrochemical cell (Figure 3.7).

  1. The cell, reference electrode and graphite were cleaned with distilled water. The electrodes were put in their position in the cell.
  2. Around 800 ml of sea water solution was put in the cell.
  3. The specimen to be tested was fitted in the working rod of the cell and placed in its position in the cell.

- Running the electrochemical test

  1. The electrochemical cell is connected to the EG&G Model 273-A potentiostat (Figure 3.7). The test, Tafel or polarization is chosen and the input data are given to the setup screen of the computer.
  2. Wait for 40 to 60 min for $E_{Corr\ r}$ to stabilize. (E_{Corr} is defined as the open circuit potential measured just prior to the start of the run.)
  3. The test was run from the setup screen. It took around one hour for the Tafel run and 10 minutes for the polarization run.
  4. Output curves and results (β_{anode}, $\beta_{cathode}$, I_{Corr}, R_p, Corrosion rate in mpy) were given in the output screen.
  5. Calculate the corrosion current (I_{corr}) and the corrosion rate (C.R) utilizing the equation; [2]

$$C.R.\ \alpha\ I_{corr} = \frac{\beta_a * \beta_c}{2.3 * (\beta_a + \beta_c)} * \frac{1}{R_p}$$

Where:

$\beta_a =$ Anodic Tafel Slope.

$\beta_c =$ Cathodic Tafel Slope

$R_p =$ Polarization Resistance

The Tafel test was done only once for each coating condition to obtain Tafel constants β_{anode} and $\beta_{cathode}$ [15]. β_{anode} and $\beta_{cathode}$ values were used in the linear polarization runs. The input data for Tafel and polarization runs are given in Table 3.3. Sample Tafel and polarization curves are given in Figures 3.8(a) and 3.8(b).

Table 3.3. Input data for Tafel and linear polarization of the electrochemical techniques.

	Input Data	
	Tafel	Polarization
Minimum Potential	-0.25 V	-0.1 V
Maximum Potential	+0.25V	+0.1 V
Scanning rate	0.16 mV/s	0.16 mV/s
β_{anode}	-	From Tafel test
$\beta_{catghode}$	-	From Tafel test
Sample Area	Depend on the sample	Depend on the sample
Sample Density	8.51	8.51
Equivalent weight	26.41	26.41

Figure 3.7 Photograph of EG&G Model 273 potentiostat.

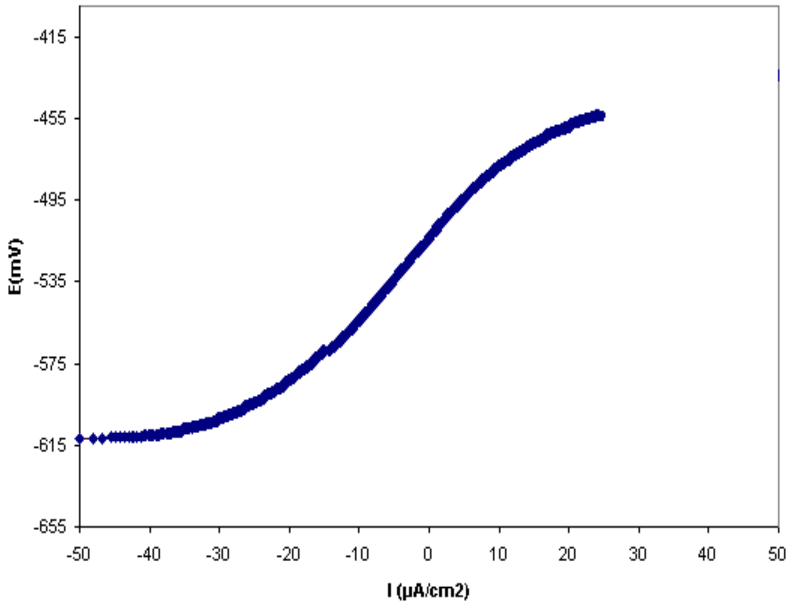

Figure 3.8(a). Sample plot of linear polarization resistance (lpr) for coating 1.

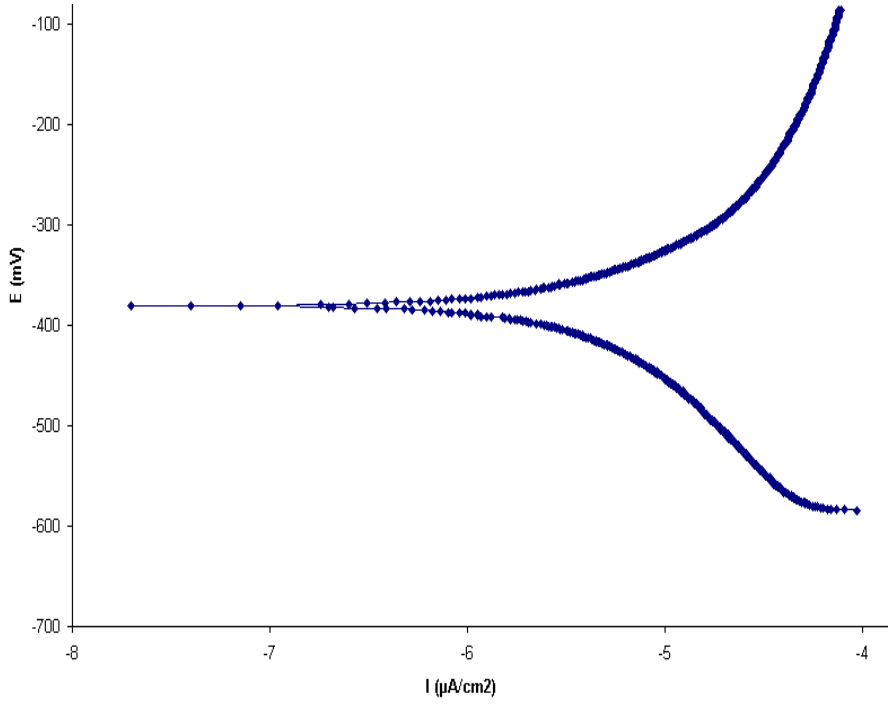

Figure 3.8(b). Sample plot of Tafel polarization for bulk material (Inconel-625).

3.7 JET IMPINGEMENT TEST PREPARATION

Erosion tests were carried out in a 1% sand contaminated seawater impingement jet at velocity of 40 m/s, temperature of 50^{o}C and pressure of 200 psi and 250 psi after heating, (Figure 3.9). This test simulates the effect of particles and fluid high flow on the solid HVOF coated surfaces at the worst summer temperature. Special Teflon holders were fabricated to ensure the prevention of any anticipated leakage. The timing of the first run was one day (24 hours) and the second run was 11 days (264 hours). Microscopic analysis using scanning-electron microscopy (SEM) were performed to characterize changes in the microstructure of the four different coatings after erosion. In addition, weight loss measurement was considered to provide a measure for the amount of material loss that each coating could produce based on its spray parameters.

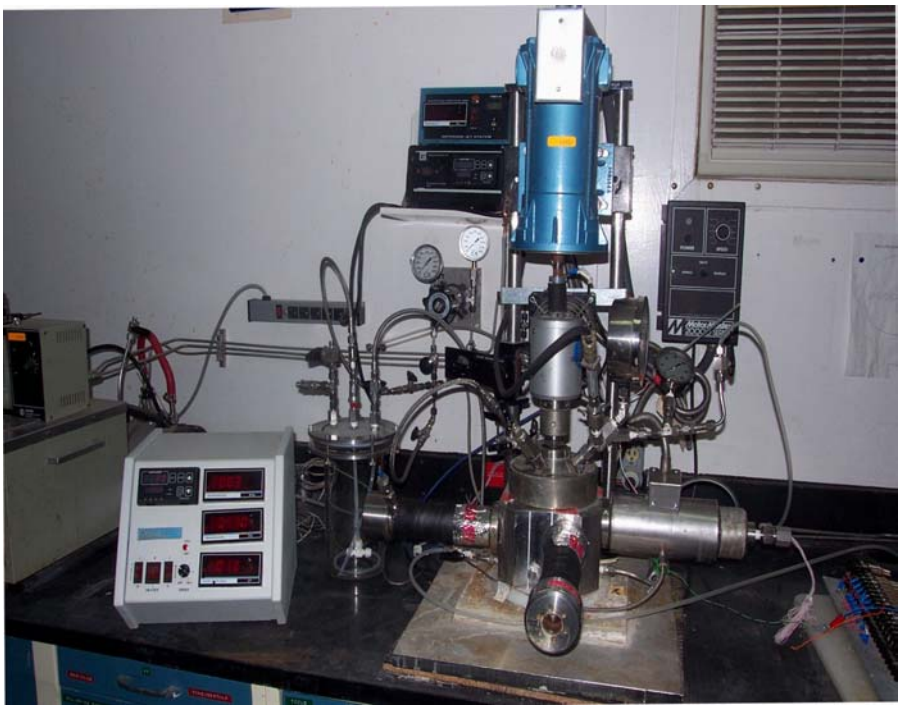

Figure 3.9 Photograph of jet impingement testing machine.

3.8 TENSILE BOND STRENGTH

The tensile bond strength evaluates the degree of adhesion of a thermally sprayed coating to a substrate. The test was conducted as per ASTM C 633 standard. The test consists of coating jointly two cylindrical specimens same base material used, one specimen is coated and the other not by an adhesive epoxy of tensile strength exceeding 12,000 Psi to ensure the failure of the HVOF coating before the adhesive, (Figure 3.10).

The test specimen is 1 inch diameter and the thickness of the applied coating is 0.020 inches that comply with the used standard. The surface of the coated and the non-coated specimen prepared mechanically using SiC paper (Grade 60). During the grinding process water was used as lubricant and cleaner. The prepared specimen was cleaned using acetone to remove any contamination.

The adhesive epoxy used is Ultrabond 100 that could resist up to 12,000 Psi if prepared and cured properly. To have full cure, the sample are exposed to high temperature for certain period of time, while maintaining the contact pressure applied. Full cure is obtained upon exposure of the sample to 150^{o}C for 80 min. The two joined specimen are hold using a newly fabricated and modified Aluminum holder that hold both specimen aligned vertically.

The test is conducted using INSTRON 8807 tensile testing machine. The machine clamping on the specimen is hydraulic, that requires precise alignment of the samples. Concentricity check for all samples are performed to ensure having zero misalignment and whenever there is misalignment, it is removed using lathe machine.

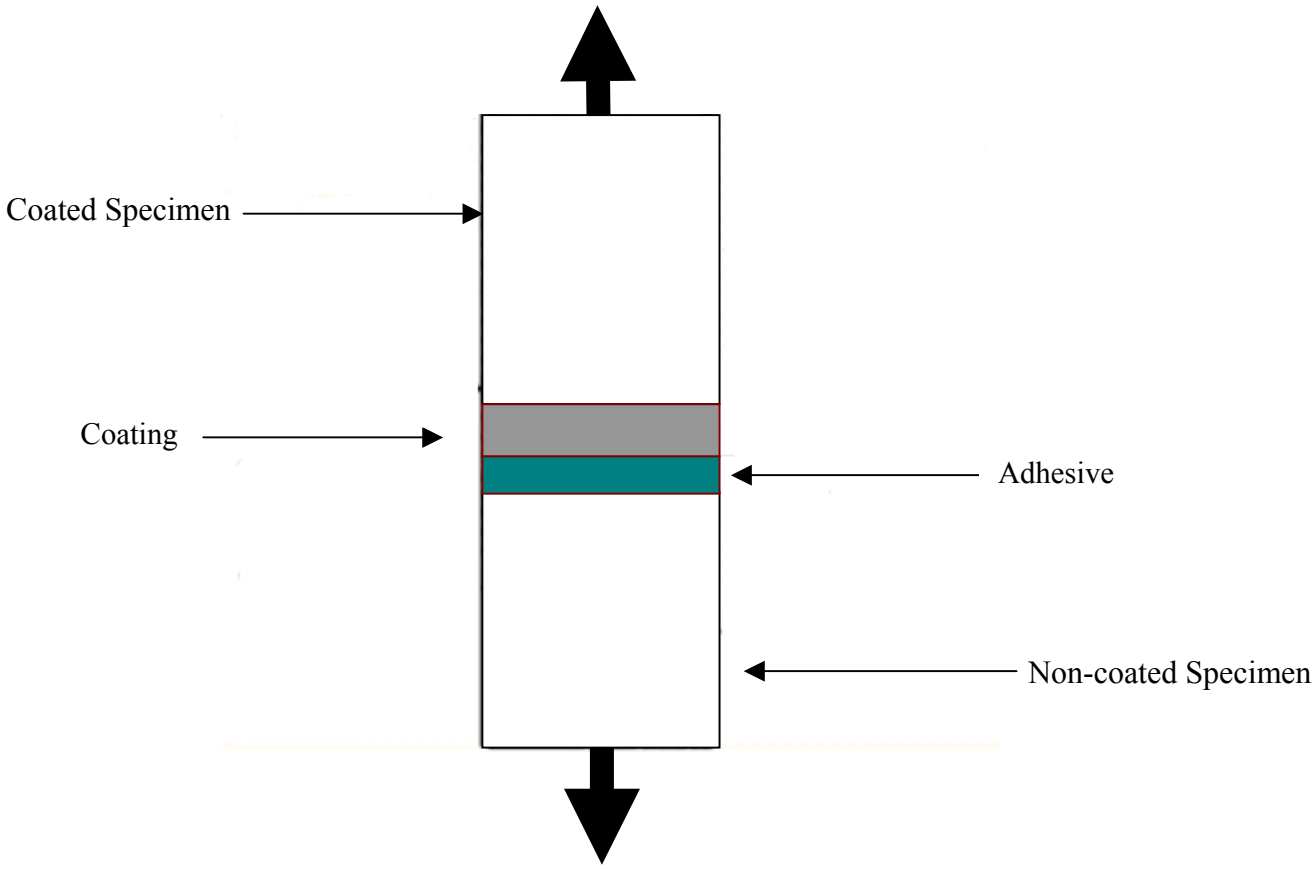

Figure 3.10 Schematic diagram of the HVOF coated specimen for tensile bonding test.

3.8.1 Testing Specimen Preparation

In the work done in this thesis all test specimens were designed in a way to adopt this kind of test. From such a setup it was too easy to get more than one sample sprayed at the same time Figure 3.11. The coating thickness was 0.020 inches which comply with the standard used. After spraying, the coated specimen were prepared by making fine grit blasting and then cleaning both surfaces coated and non coated by acetone to take out any contamination.

3.8.2 Bonding Adhesive

An adhesive epoxy that could exceed 12,000 psi was not available with many adhesive manufacturers. The epoxy used in this test was a German made epoxy (HTR Ultrabond 100) manufactured by HTR Hamburg GMBH, with a tensile strength exceeding 14,000 psi. To have full curing of the adhesive, the samples were exposed to high temperature 190^{o}C for 35 min. The rate of tensile load was between 0.013 mm/s to 0.021 mm/s.

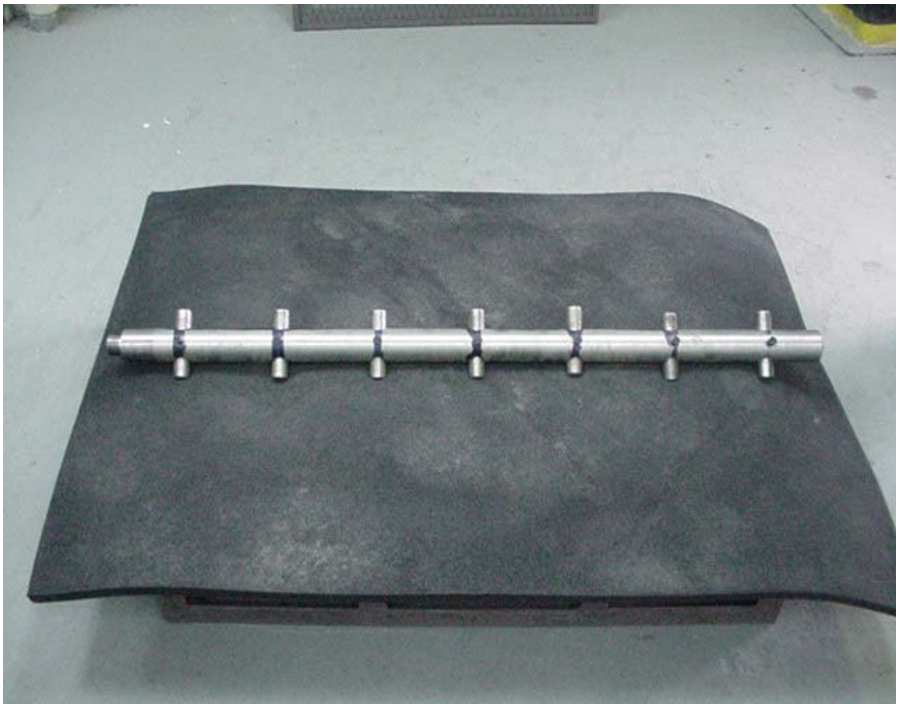

Figure 3.11 Preparation setup of the sample for tensile bond strength.

Chapter 4

RESULTS

4.1 COATING MICROSTRUCTURE ANALYSIS

Many spray parameters could affect the coating microstructure. These could be either surface preparation parameters such as grit type, blasting conditions, grit feed rate and sample surface roughness or operational parameters such as powder feed rate, stand- off distance, gun pressure, workpiece transfer speed, output energy and work piece surface temperature.

In the present study, only two parameters were varied, the stand off distance and the powder feed rate. The reason why we have selected these two parameters is that these are the only ranged parameters as per the manufacturer specification, while the rest are all fixed. The given range of the stand-off distance is (9 inches to 12 inches) and for the powder feed rate is (5Ib/h to 20Ib/h).

4.1.1 Porosity

Specimen was prepared for porosity test by cutting the sample in half using a diamond cutoff wheel. Care was taken to insure that the cutting wheels engages first into the

coating then the substrate to avoid detaching. The sectioned specimen was embedded in the resin for mounting. The samples were then grounded and polished using ECOMET3 disc at rotational speed of 120 rpm and using water as a lubricant. The time at each step was three to four minutes. Each coating condition has two identical samples for each microstructural analysis. The porosity quantification was done for each case separately.

Porosity was quantified using the image analysis software integrated with the electron microscope. This was done through capturing the digital image of the coated sample using the backscattered electron detector and optimizing the gray levels of the sample surface defects such as porosity.

Coatings 1 and 2 were sprayed applying low powder feed rate 5 lb/h with different spray distances (Table 3.2). Variation of the porosity on both coatings is shown in Figures 4.1(a, b) and 4.2(a, b). Coatings 3 and 4 were sprayed applying high powder feed rate 20 Ib/h with different spray distances as shown in Figures 4.3(a, b) and 4.4(a, b). A summary of two runs for porosity measurements with the four different coatings is shown in Table 4.1. Figure 4.5 shows the porosity variation with powder feed rate. It is observed that as the powder feed rate increase coating porosity increase. Figure 4.6 shows the porosity variation with the spray distance. It is noted also that as the spray distance increases porosity increases, and it was also shown that the powder feed rate variation is the determining factor of porosity change. An area of (200µm x 200µm) was selected for image analyzer measurements to ensure representative data (Figure 4.7).

Figures 4.8(a, b, c, d) show random variation of porosity with coating thickness that vary from 300µm to 500µm. Figure 4.8 does not show significant dependence of porosity

with thickness. Note that this variation of coating buildup might result from the variation of the coating build up rate during spraying process. Porosities within the coating have distribution of sizes and could vary from (5.0 μm x 10 μm) to (6.0 μm x 21.0 μm) as shown in Figure 4.9.

Table 4.1. Porosity readings of the coated samples

Coating	Run 1 Porosity %	Run 2 Porosity %	Average
1	2.1	1.8	1.95
2	2.9	3.1	3
3	5.2	5.1	5.2
4	5.7	5.9	5.8

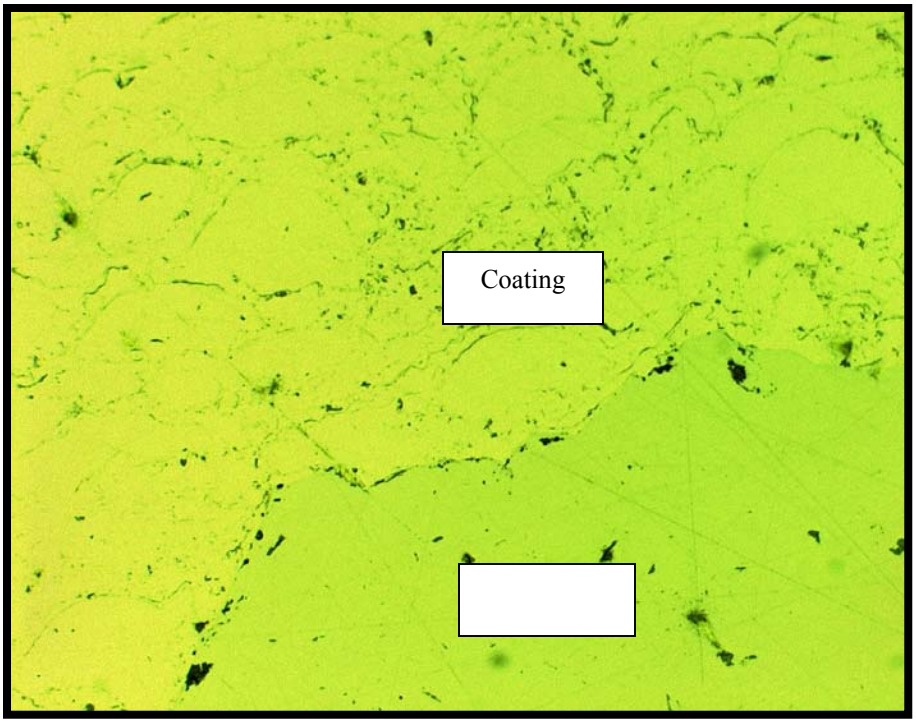

Figure 4.1(a) Optical micrograph of coating 1 (500x).

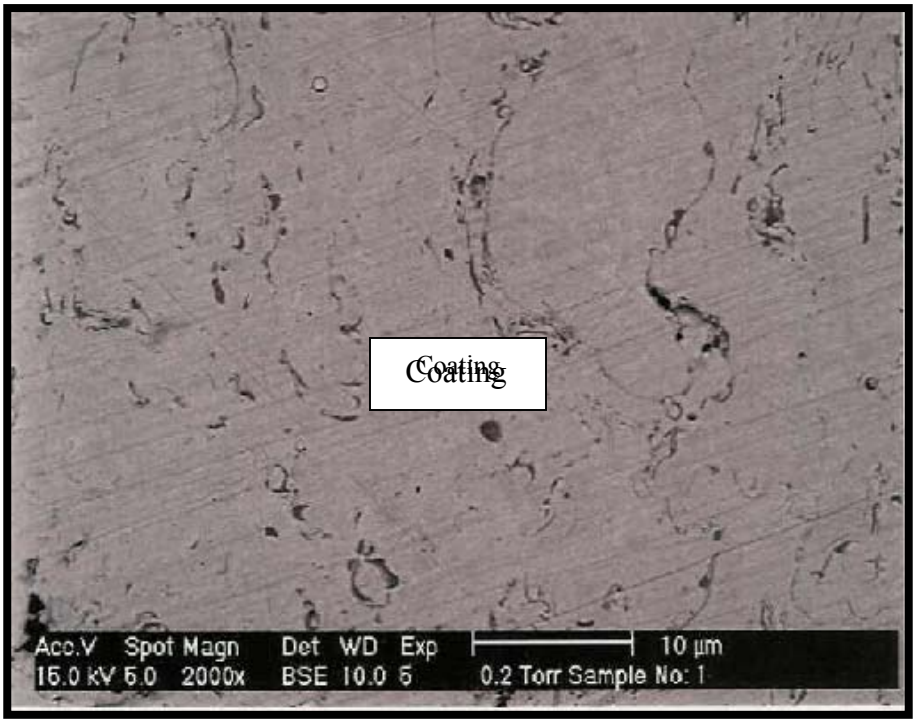

Figure 4.1(b) SEM image of coating 1 (2000x).

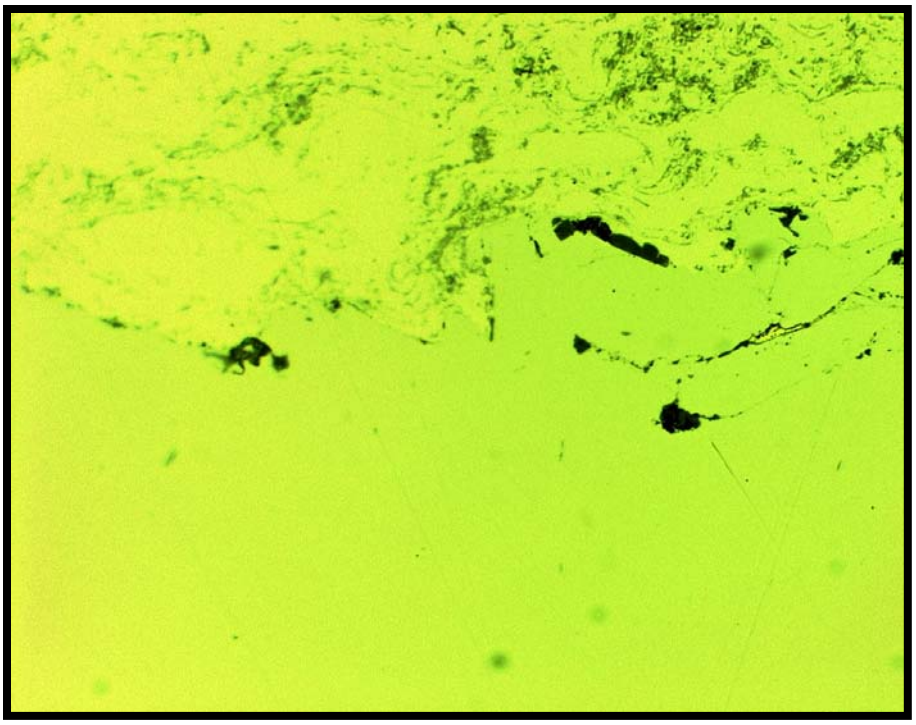

Figure 4.2(a) Optical micrograph of coating 2 (500x).

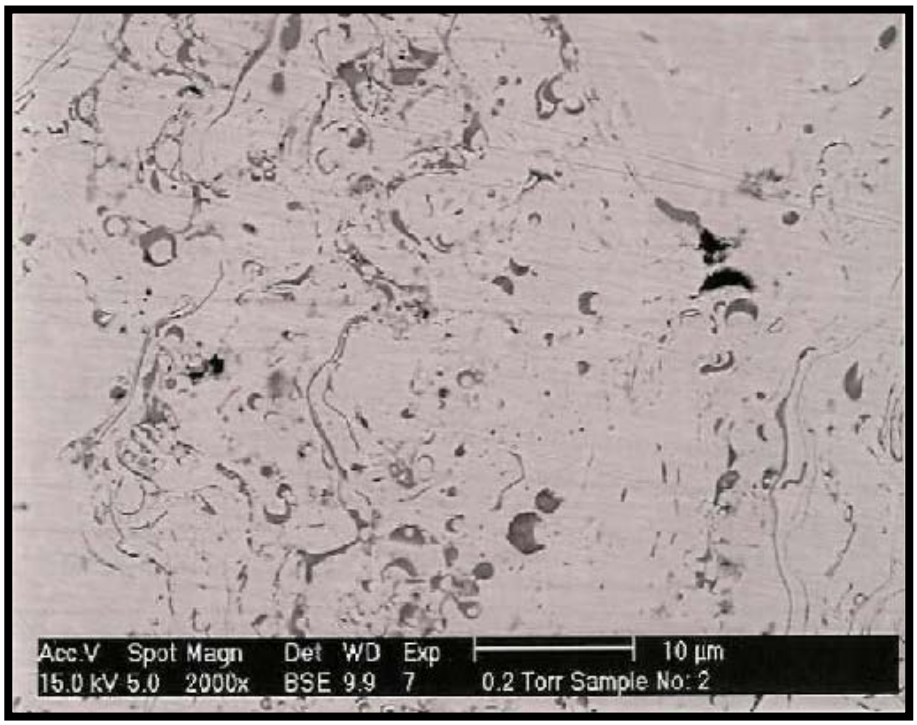

Figure 4.2 (b) SEM image of coating 2 (2000x).

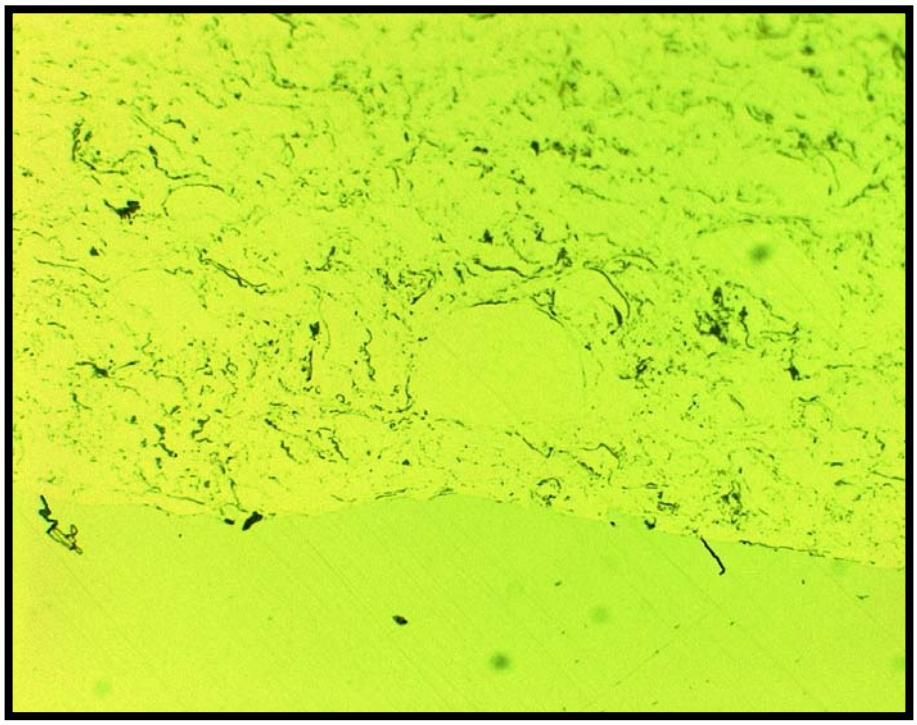

Figure 4.3(a) Optical micrograph of coating 3 (500x).

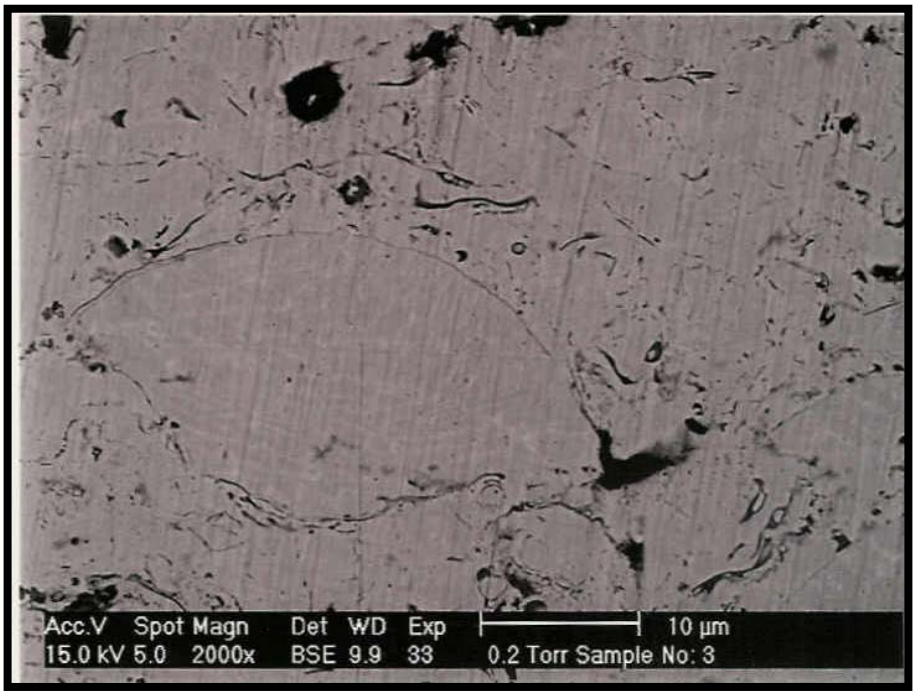

Figure 4.3(b) SEM image of coating 3 (2000x).

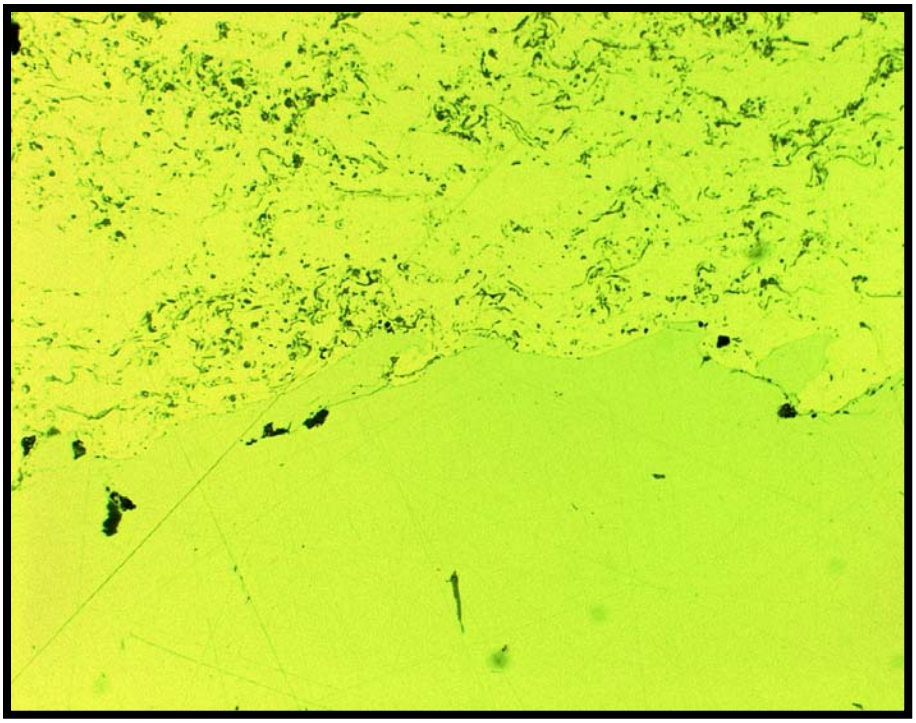

Figure 4.4(a) Optical micrograph of coating 4 (500x).

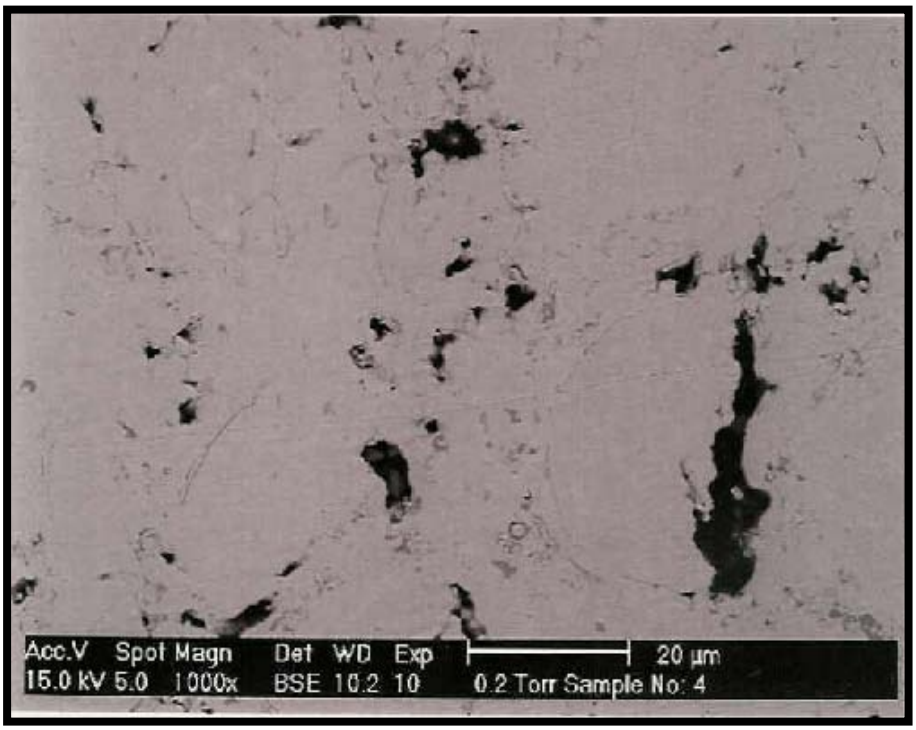

Figure 4.4(b) SEM image of coating 4 (2000x).

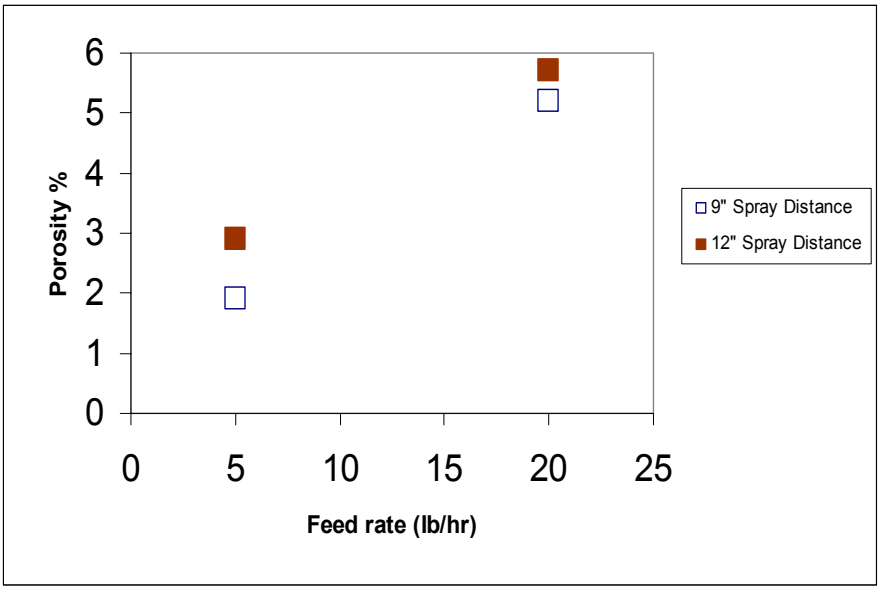

Figure 4.5 Porosity variation vs powder feeding rate.

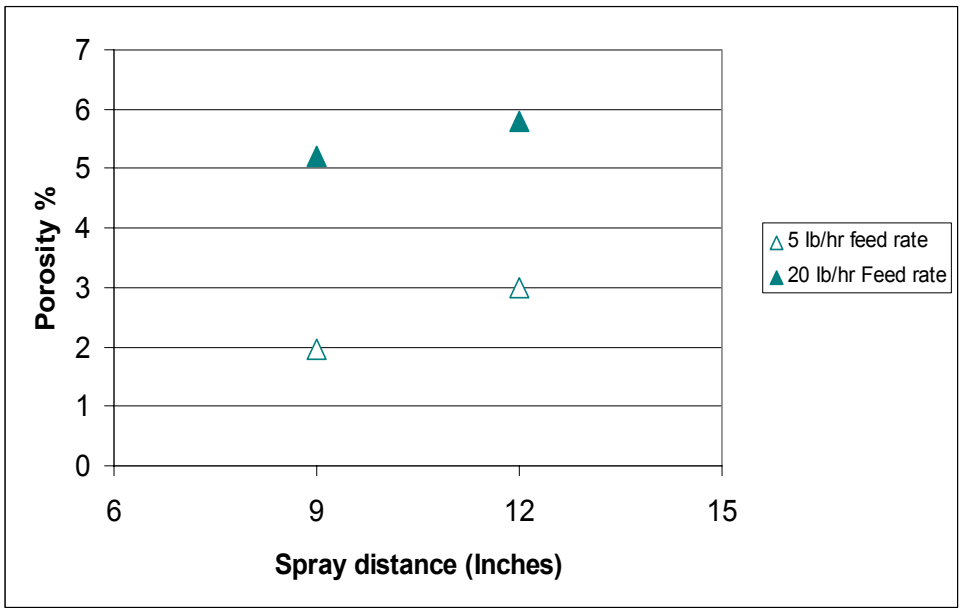

Figure 4.6 Porosity variation vs stand-off distance.

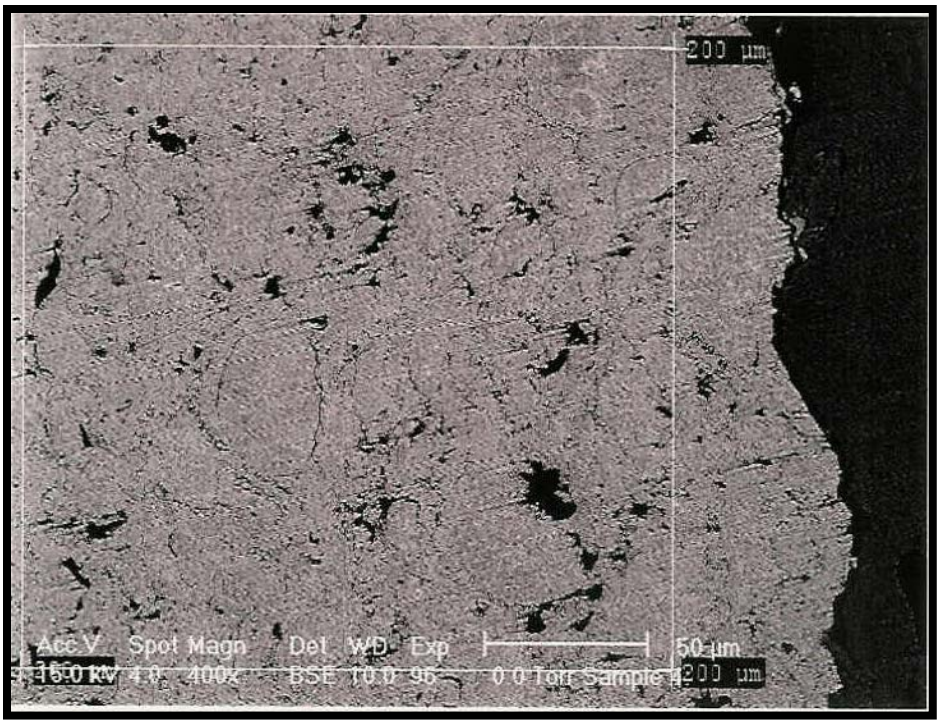

Figure 4.7 SEM image of the area of the measured porosity (200 µm X 200 µm) for coating 4.

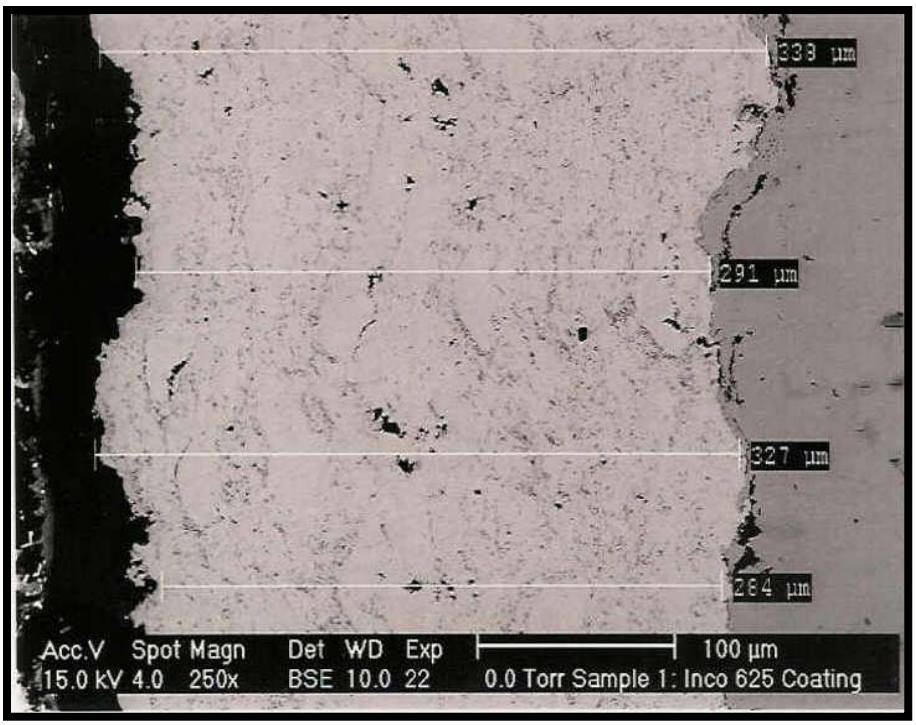

Figure 4.8(a). SEM image of the change of porosity with thickness for coating 1.

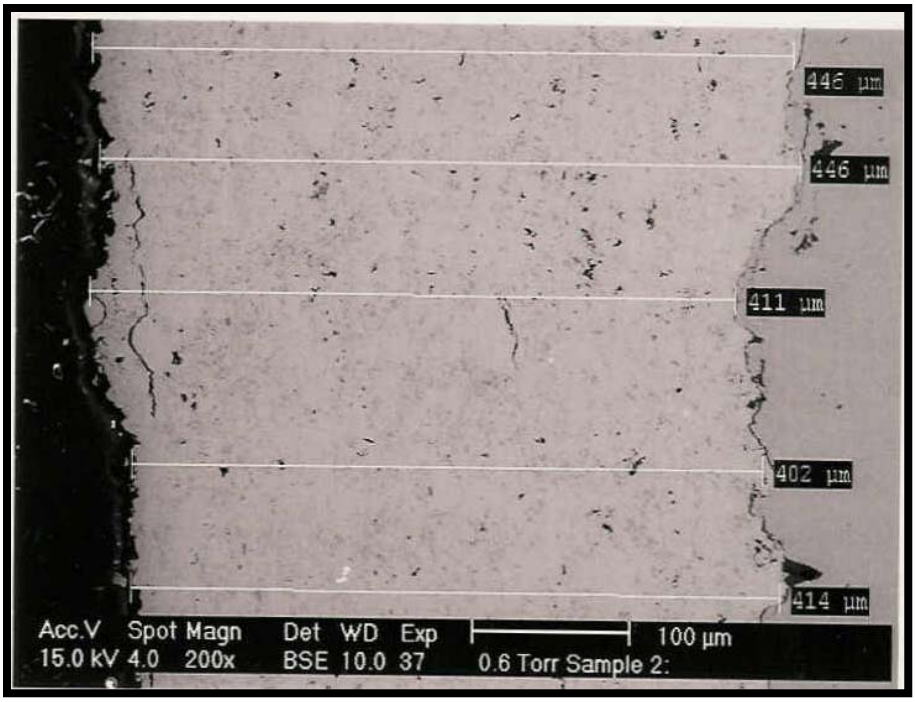

Figure 4.8(b). SEM image of the change of porosity with thickness for coating 2.

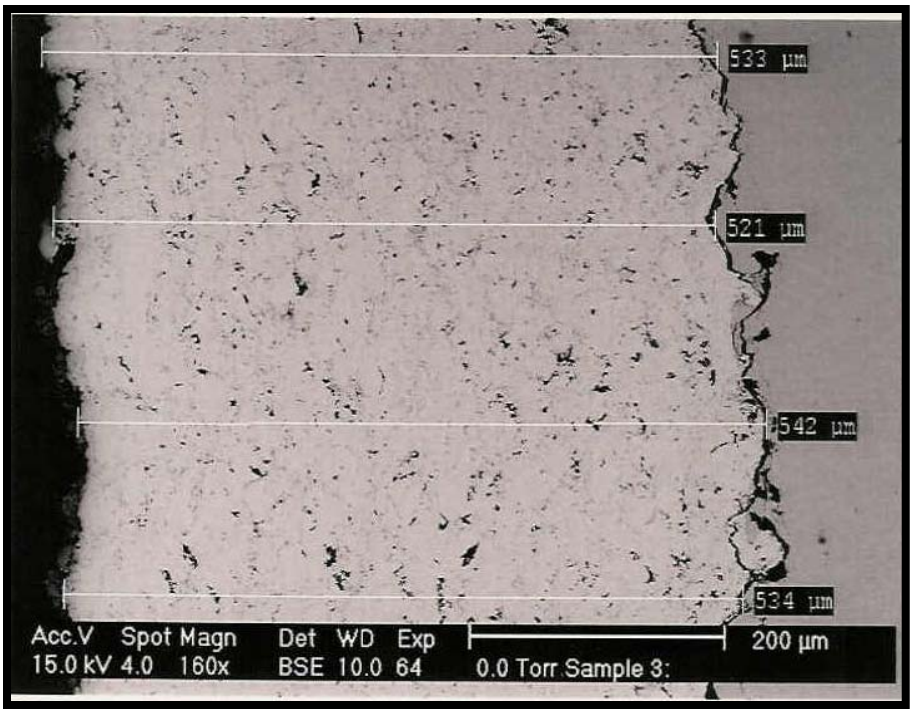

Figure 4.8(c) SEM image of the change of porosity with thickness for coating 3.

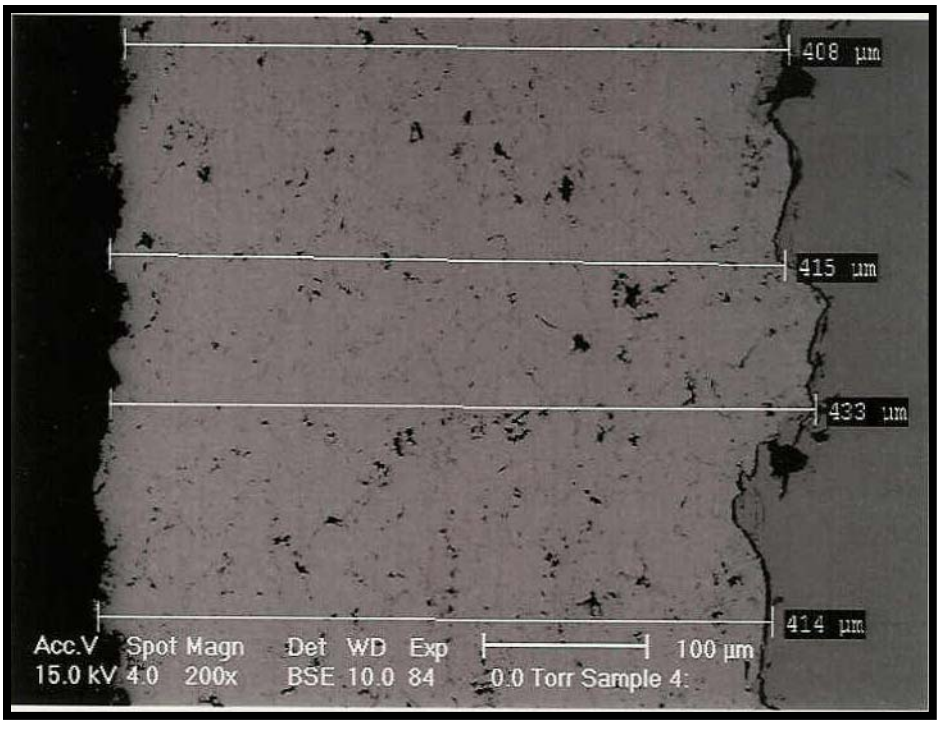

Figure 4.8(d) SEM image of the change of porosity with thickness for coating 4.

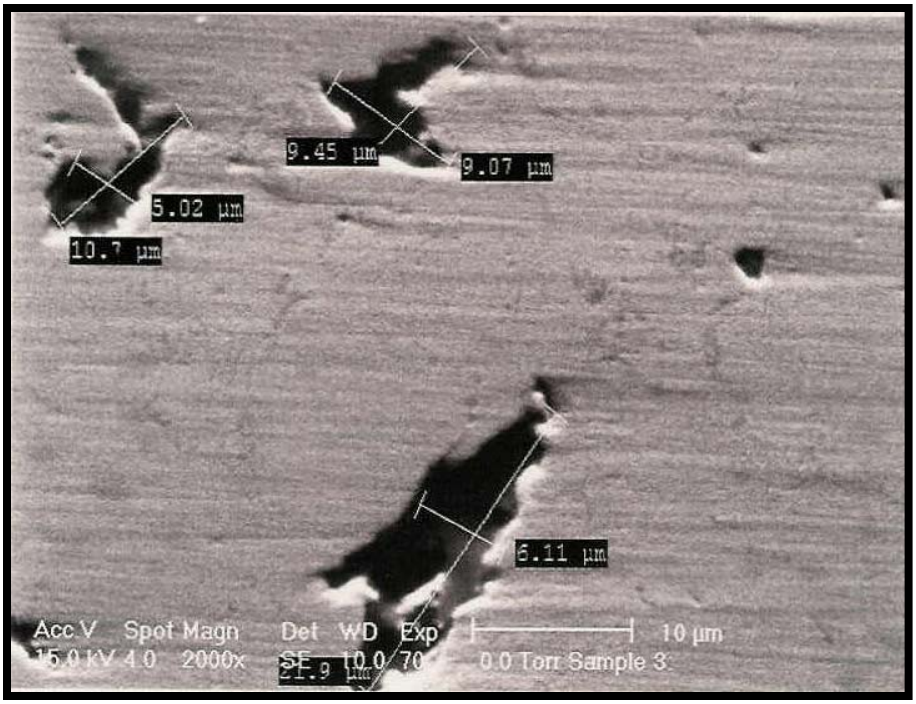

Figure 4.9 SEM image showing the porosity sizes for coating 3 at 2000x.

4.1.2 Oxidation Test Results

Oxygen content on the coating has a great effect on the coating integrity. Different setting parameters may produce different oxygen content. Oxygen content was estimated using a semi quantitative analysis of the energy dispersive spectrometer (EDS), Model Xl-30 by EDAX attached to the Philips scanning electro microscope, model XL-30.

Three different readings were taken for coating 1 with approximate area of (17.1 x 15.1) μm^2 and all shows similar results (average oxide content of 4.2 wt%). Due to the high work load on the machine (EDS analyzer), the oxide content for coating 2, 3 and coating 4 were measured only twice. A flat polished sample was analyzed. Since the oxygen atomic weight is very small in comparison with iron (Fe), chromium (Cr)…etc, this technique of analysis will quantify the oxygen with minimum accuracy through other elements like iron Fe, Cr, Ni…etc will have high accuracy. It is thought that the oxide in the coating is primarily chromium oxide (Cr_2O_3), (Figures 4.10-4.13).

4.1.2-1 Spray Distance

In coatings 1 and 3 the spray distance was 9 inches, and it shows low oxidization content, (Figure 4.10 & 4.12). However, Figures 4.11 & 4.13 show a slight increase of the oxide content in the coating sprayed at 12 inches. This indicates that as the spray distance increases, coating oxide content increases.

4.1.2-2 Powder Feed Rate

A summary of two run for coating oxide content variation is shown in Table 4.2. Figure 4.14 shows that the stand off distance is the more influencing parameter on coating oxidization. Figure 4.15 shows that there is a slight variation on the oxide content if powder feed rate were changed. It is noted that as both spray distance and powder feed rate increase, oxide content in the coating increase. Also, the effect of spray distance is more pronounced at low feed rate.

Table 4.2. Oxygen content in the coated samples.

Coating	Run 1 Oxide Content Wt %	Run 2 Oxide Content Wt %	Average Oxygen Content Wt %
1	4.2	4.1	4.15
2	8.0	8.2	8.1
3	7.1	6.9	7
4	9.5	9.3	9.4

4.1.2-3 Coating Structure Change

Electrochemical etching on the coating surface shows that, the coating internal structure is changing from coating to another according to the sprayed parameters (Figure 4.16 (a, b)). This variation in the structure could be related to porosity content as well fraction of unmelted particles. The complex morphology of the coating buildup made quantitative optical analysis questionable.

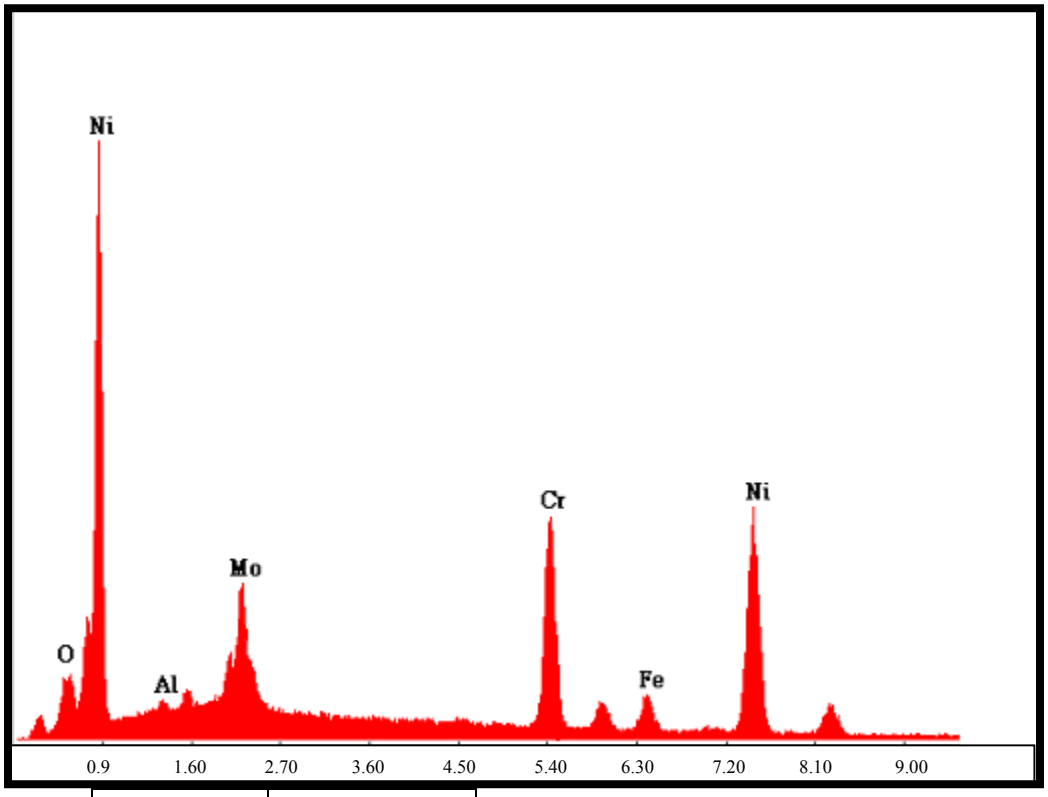

Element	Average Wt %
O	04.15
Mo	10.04
Cr	20.14
Fe	05.52
Ni	60.10
Total	100.00

Figure 4.10 Amount of oxide in coating 1 "(17.7x15.1) μm^2 area analysis: 2000x".

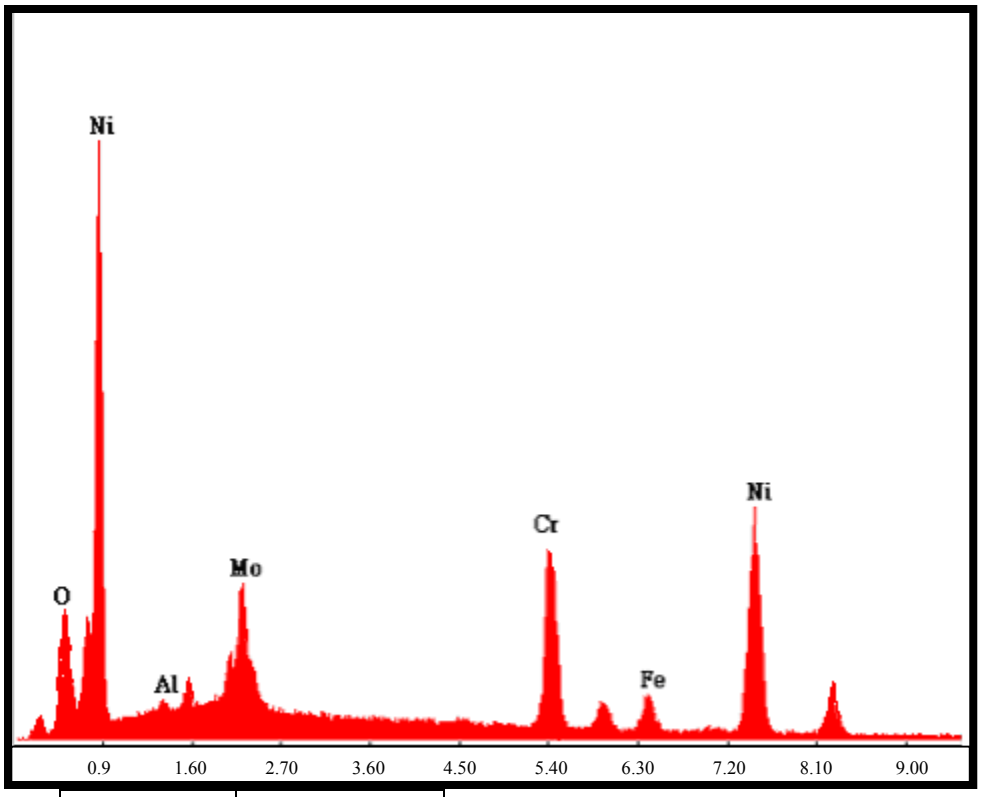

Element	Average Wt %
O	08.10
Mo	08.81
Cr	18.89
Fe	04.99
Ni	59.10
Total	100.00

Figure 4.11 Amount of oxide in coating 2 "(17.7x15.1) μm^2 area analysis: 2000x".

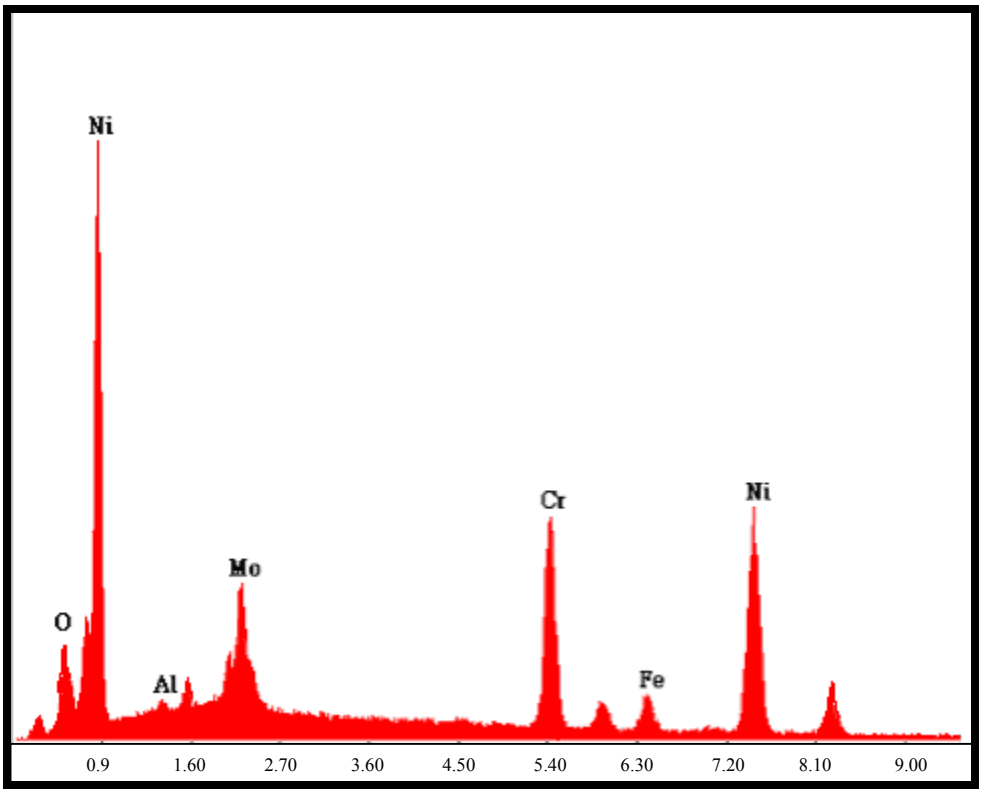

Element	Average Wt %
O	07.00
Mo	09.15
Cr	19.20
Fe	05.00
Ni	59.85
Total	100.00

Figure 4.12 Amount of oxide in coating 3 "(17.7x15.1) μm^2 area analysis: 2000x".

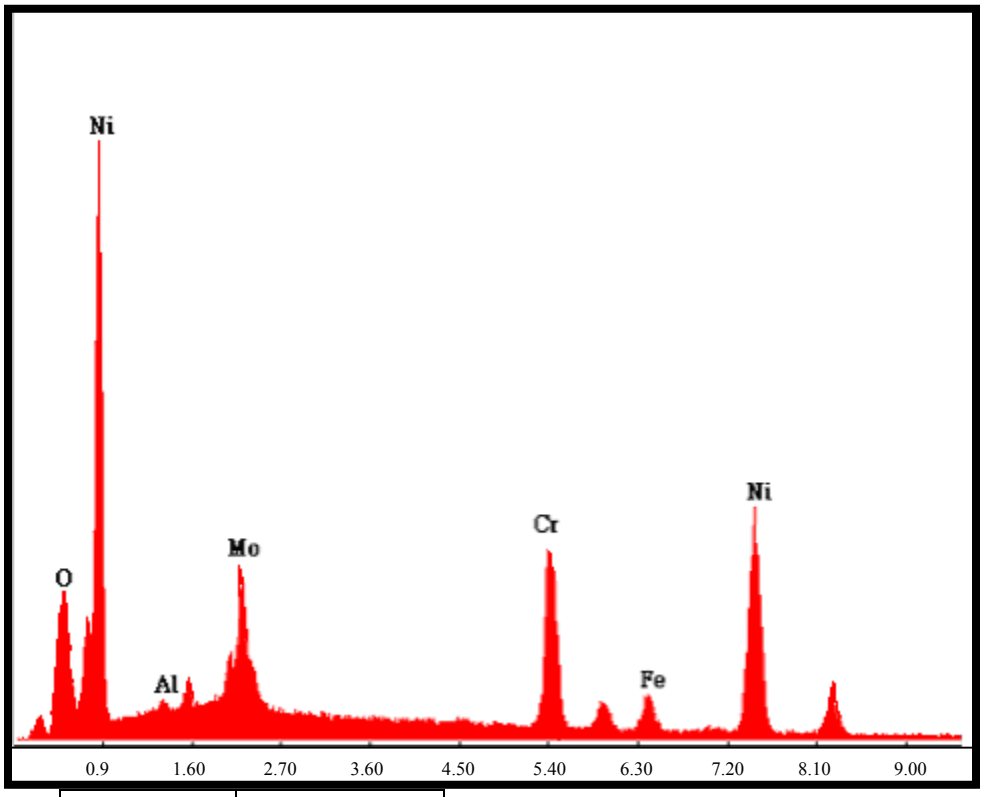

Element	Average Wt %
O	09.40
Mo	10.10
Cr	15.30
Fe	05.10
Ni	60.00
Total	100.00

Figure 4.13 Amount of oxide in coating 4 "(17.7x15.1) μm^2 area analysis: 2000x".

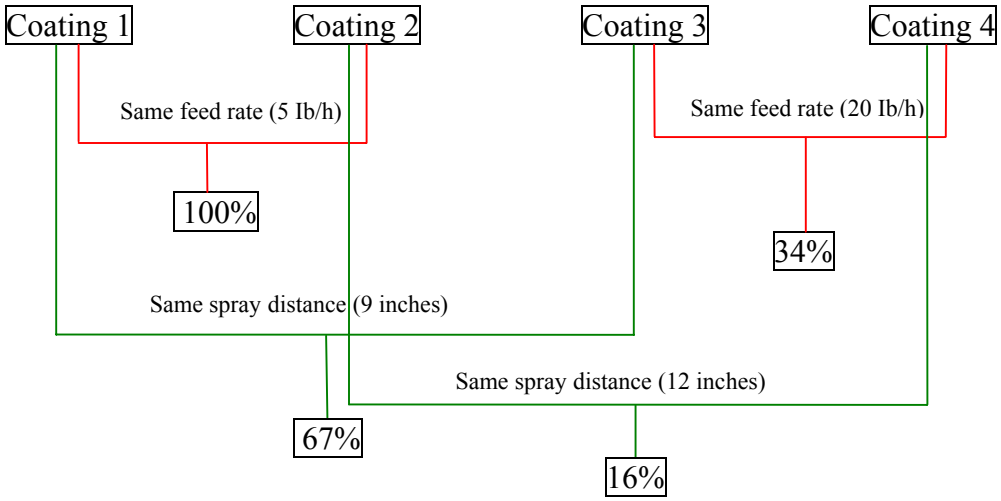

Figure 4.14 Summary of comparison between the spray distance and the powder feed rate effect on oxidization.

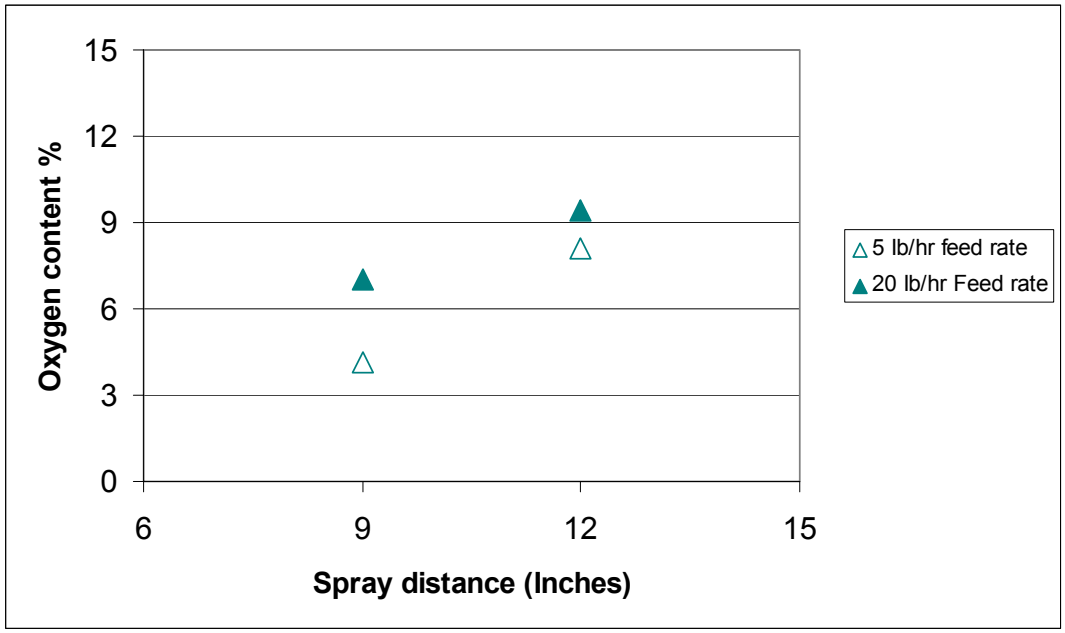

Figure 4.15 Variation of coating oxygen content with spray distance.

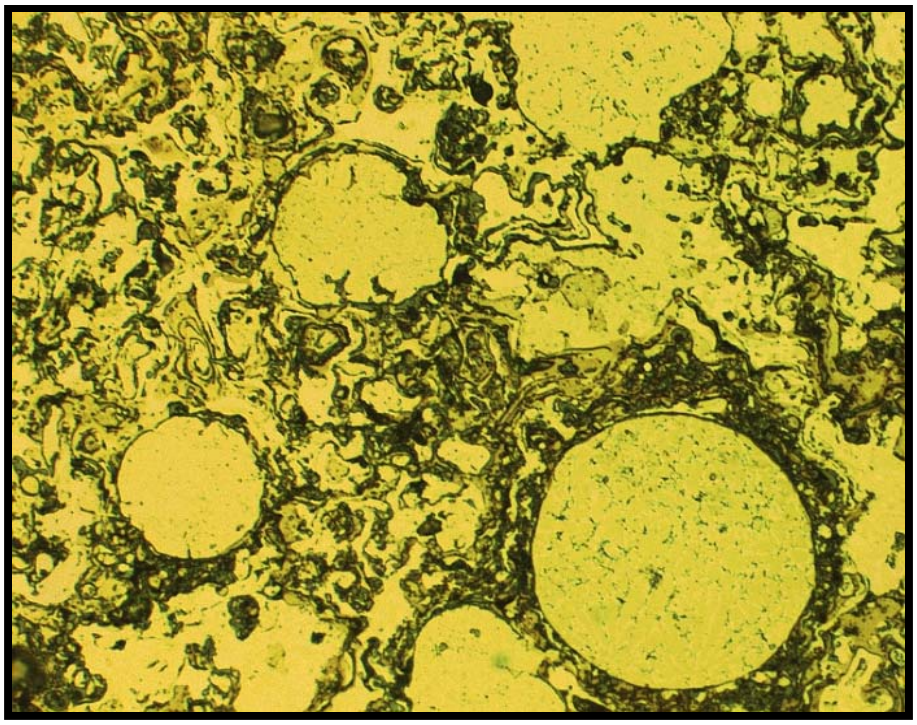

Figure 4.16(a) Optical micrograph of electrochemical etched surface of coating 2. 500x.

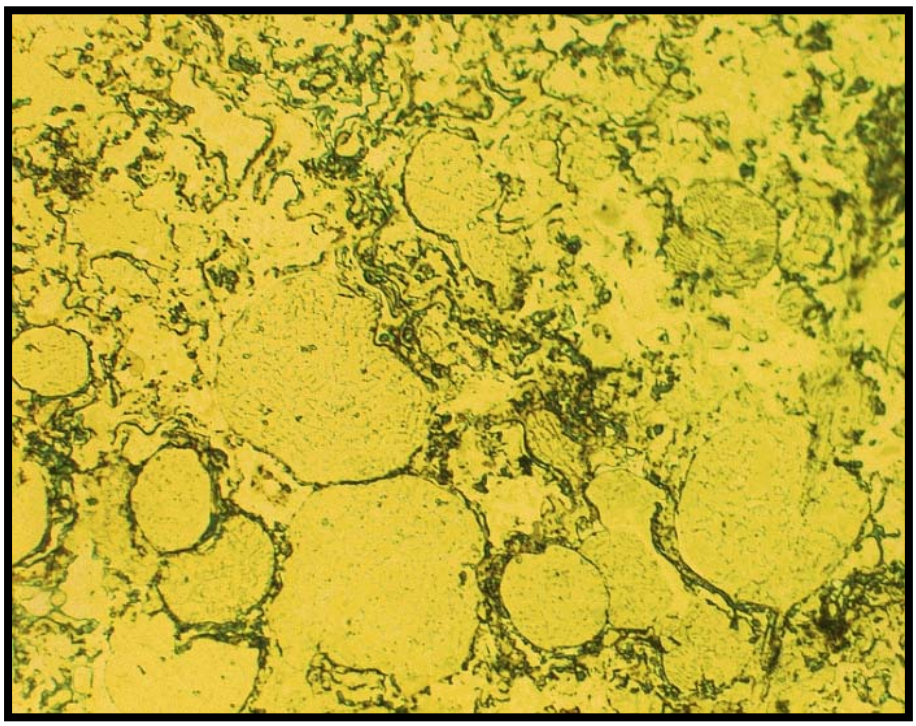

Figure 4.16(b) Optical micrograph of electrochemical etched surface of coating 3. 500x.

4.2 MICROHARDNESS TEST RESULTS

4.2.1 Variation of Microhardness Along Coating Thickness

Microhardness test was performed with a 500 g test load and it was taken in the same samples used for porosity quantification, in which both have the same surface preparation mentioned before. Figure 4.17 shows the locations of microhardness test indenter for all coated samples. The microhardness reading of each coating is shown in Table 4.3. Figure 4.18 shows variation of microhardness with coating thickness. An average of the three points (1, 4, 7), (2, 5, 8) and (3, 6, 9) were considered for the microhardness variation along thickness for the four coatings. It is noted that as we go far from the substrate, coating microhardness decrease for all examined coatings.

Table 4.3 Microhardness readings for the four coated samples (Vicker).

	1	2	3	4	5	6	7	8	9	Avg.	Stan. Dev.
Coating 1	445	440	421	450	443	419	448	443	418	436	13
Coating 2	438	426	404	439	428	403	438	423	402	422	15
Coating 3	405	397	340	410	385	396	408	378	395	390	21
Coating 4	330	315	300	318	313	298	316	336	301	317	12

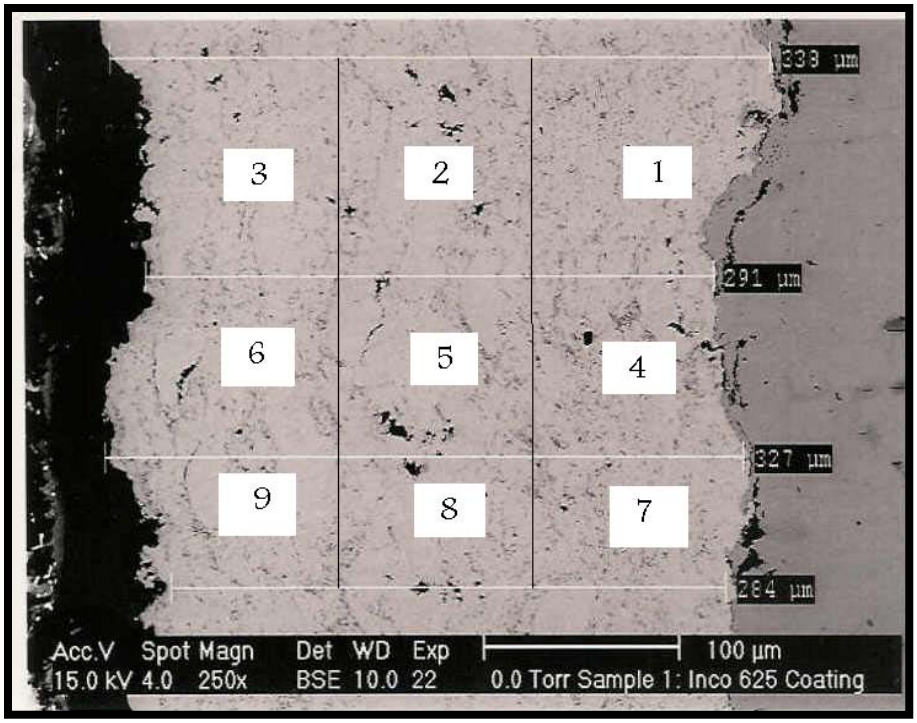

Figure 4.17 Location of the microhardness indenter for coating 1 (300 µm x 300 µm).

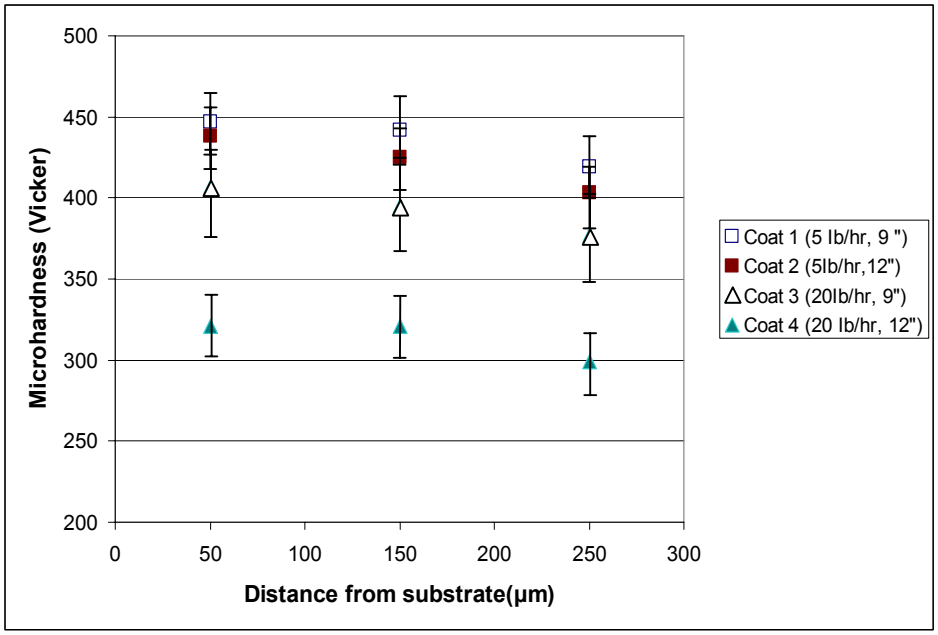

Figure 4.18 Variation of microhardness with coating thickness.

4.2.2 Microhardness Variation with Spray Distance

Coating 1 and coating 3 were sprayed at minimum spray distance (9 inches) while coating 2 and coating 4 where sprayed at maximum spray distance (12 inches). Figure 4.19 shows that as the spray distance increased, the measured microhardness decreased for the same feed rate. This behavior can be clearly seen when comparing coatings 1 and 2; and coating 3 and 4.

4.2.3 Microhardness Variation with Powder Feed Rate

Coating 1 and coating 2 were sprayed at minimum powder feed rate (5 Ib) while coating 3 and coating 4 where sprayed at maximum powder feed rate (20 Ib). Figure 4.20 shows that as the powder feed rate increased, the resulted coating exhibited reduced microhardness at the same distance of spray. Comparison of coatings 1 and 3; and coatings 2 and 4 reveals this behavior.

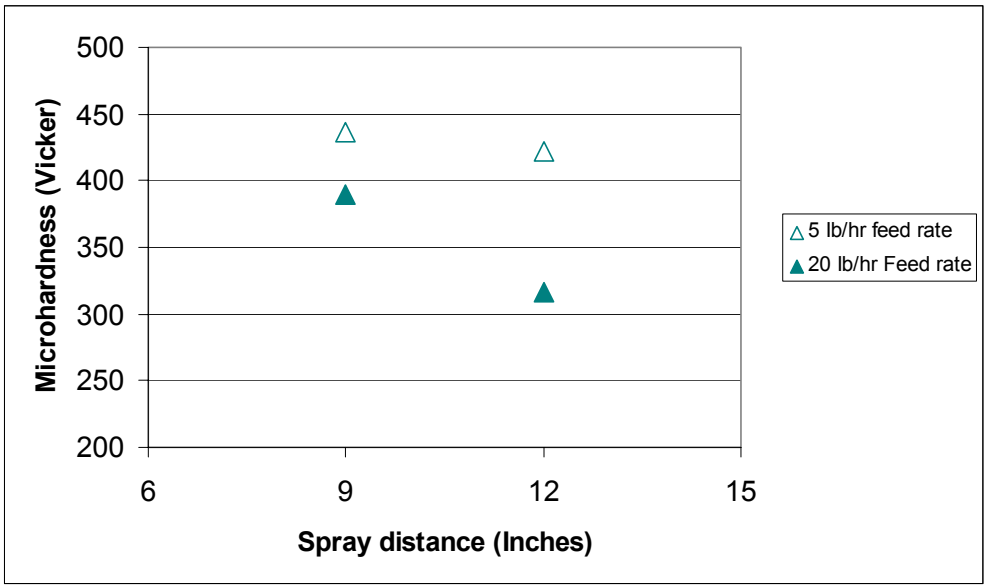

Figure 4.19 Variation of microhardness with spray distance.

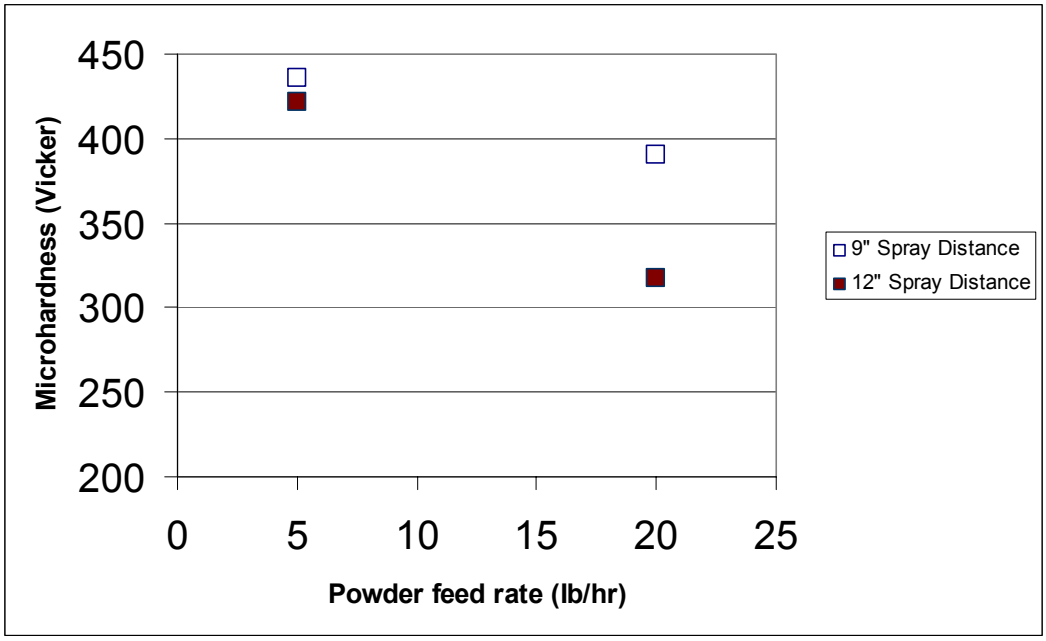

Figure 4.20 Variation of microhardness with powder feeding rate.

4.2.4 Variation of Surface Microhardness

Table 4.4 shows the surface microhardness variations for the four coatings at five different points. Figure 4.21 shows the locations were the microhardness is taken at the coating surface. Results of the measurements reveal that there is insignificant difference between the microhardness measurements at the surface of a given coating. However, as both spray distanced and powder feed rate increased, coating surface microhardness decreased as can be inferred from Figure 4.22. Results indicate that variation of the microhardness is more pronounced with variation in the applied feed rate.

Table 4.4 Surface microhardness reading for the 4 coatings.

	Point 1	Point 2	Point 3	Point 4	Point 5	Average	Stand. Dev.
Coating 1	435	442	429	451	446	440	8
Coating 2	424	412	416	423	417	418	5
Coating 3	390	385	397	401	387	392	6
Coating 4	341	334	347	348	337	341	6

Figure 4.21 Photograph showing the 5 points where microhardness is measured at the sample coating surface.

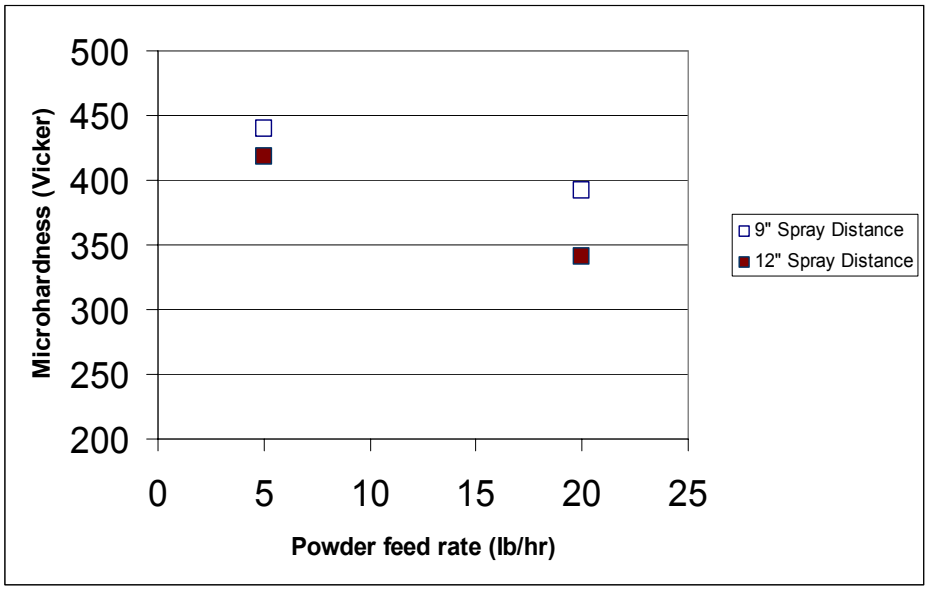

Figure 4.22 Micrhardness variation with powder feed rate at the coating surface.

4.3 CORROSION TEST RESULTS

Figure 4.23 shows the linear polarization curves for coating 1 and coating 2. The linear polarization method was utilized to determine the effect of the different spray parameters on coating corrosion resistance. Sea water was selected as the electrolyte, because most of the application of the Inconel-625 is on the corrosive environment. The corrosion test was made according to ASTM G 5. Table 4.5 lists the measured R_p and the calculated I_{Corr} for all coatings.

4.3.1 Corrosion Resistance with Spray Distance

The R_p (Polarization Resistance) value of coating 1 is more than the R_p value of coating 2. It can be shown that coating 1 is better than coating 2 in terms of corrosion resistance. Coating 1 and coating 2 both have the same powder feed rate (5 Ib/h), but they differ in the spray distance.

The plot presented in figure 4.24 shows the linear polarization of coating 3 and coating 4. The slope of both plots reveals that R_p value of coating 3 is more than R_p value of coating 4, (Table 4.5). This indicates that coating 4 has high susceptibility to corrosion than coating 3. Since both coatings have the same powder feed rate (20 Ib/h) and they differ in the spray distance only, this means that at high powder feed rate, the spray distance effect on coating corrosion is more pronounced.

4.3.2 Corrosion Resistance with Feed Rate

Figure 4.26 shows the effect of powder feed rate variation on the corrosion rate of the four different coatings in reference to the bulk material (Inconel-625 solid rod). Coating 1 and coating 2 are much better in terms of corrosion resistance than coating 3 and coating 4. It is evident that as the powder feed rate increased, the corrosion rate increased.

Table 4.5. R_p and I_{Corr} values for coatings 1-4 with values of the bulk material for reference.

Material	B_a	B_c	B	R_p	I_{Corr}
Bulk (Solid Rod Inconel 625)	0.067	0.108	0.017978	10.14	0.001773
Coating 1	0.064	0.109	0.017532	3.96	0.004427
Coating 2	0.065	0.109	0.017704	2.64	0.006706
Coating 3	0.064	0.109	0.017532	0.731	0.023984
Coating 4	0.064	0.11	0.017591	0.465	0.037831

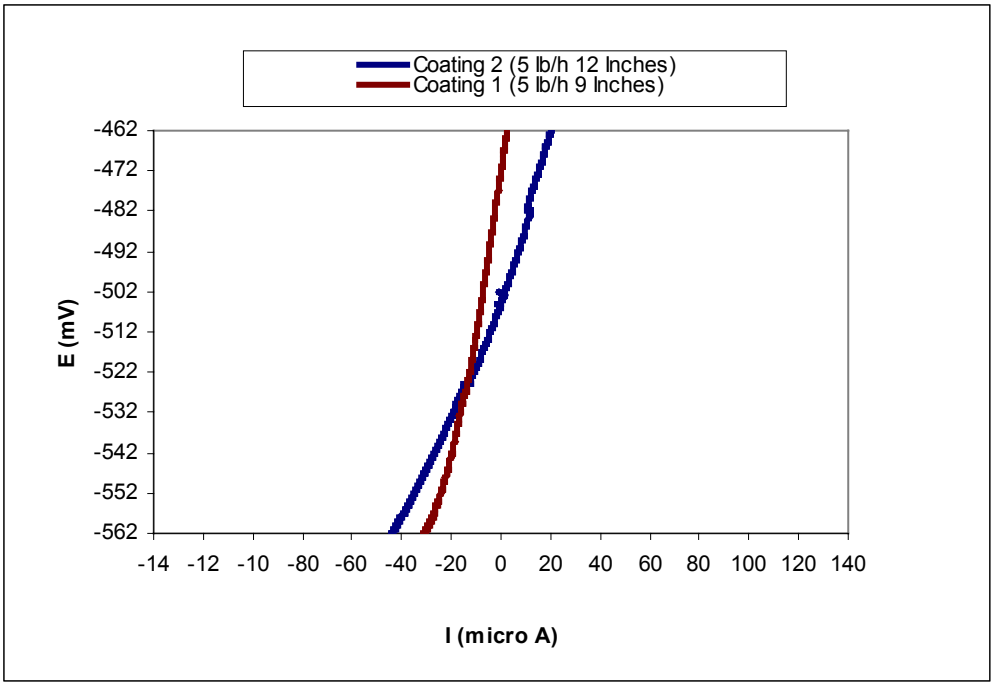

Figure 4.23 Linear polarization plot for coating 1 & 2.

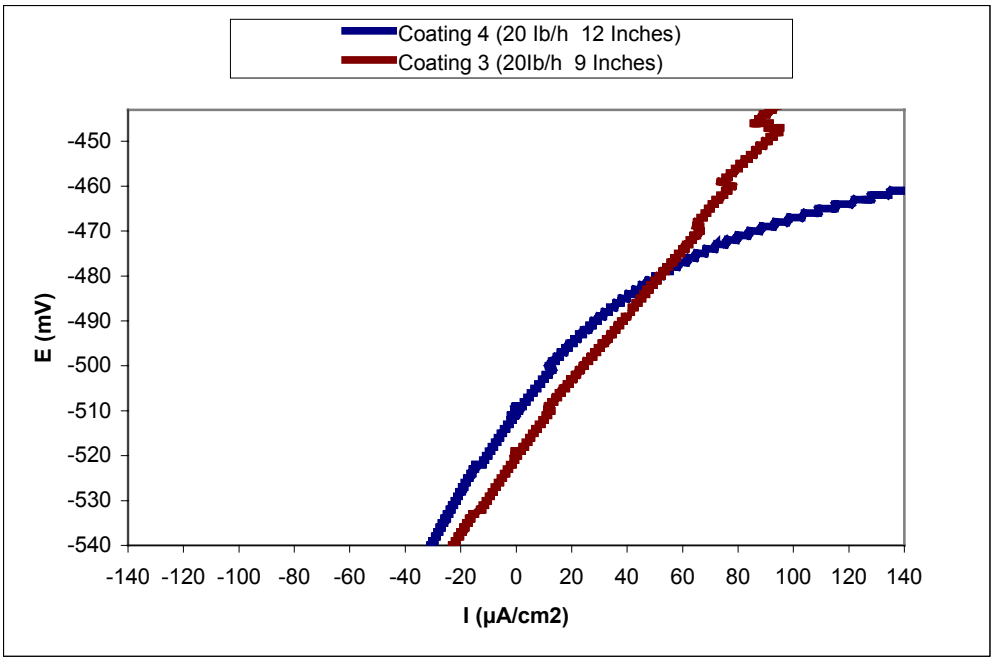

Figure 4.24 Linear polarization plot for coating 3 & 4.

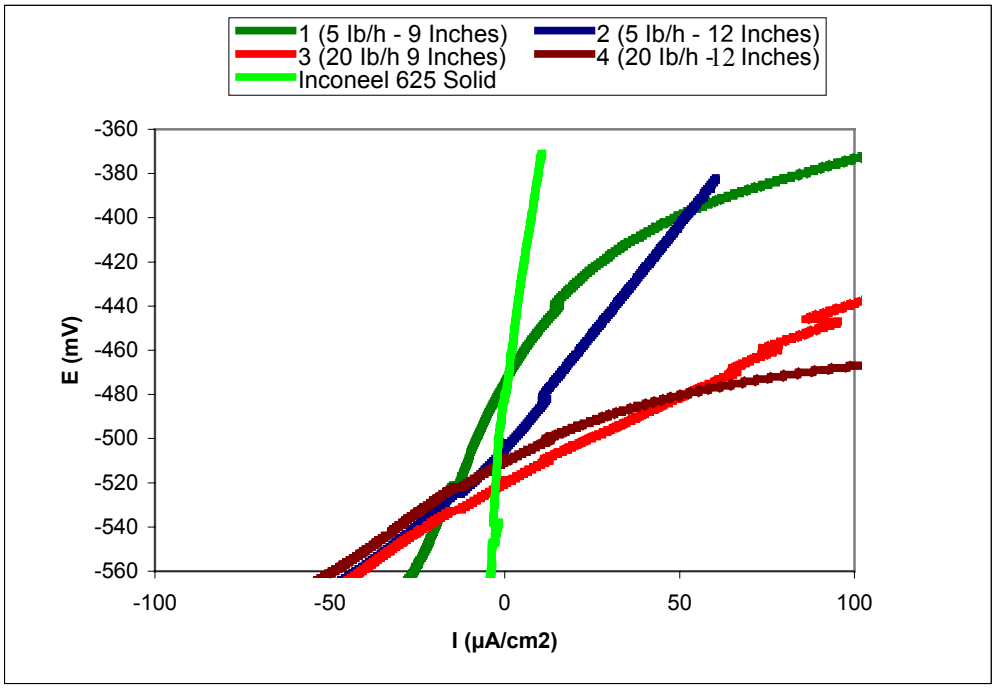

Figure 4.25 Linear polarization plots for all coatings in reference with the bulk

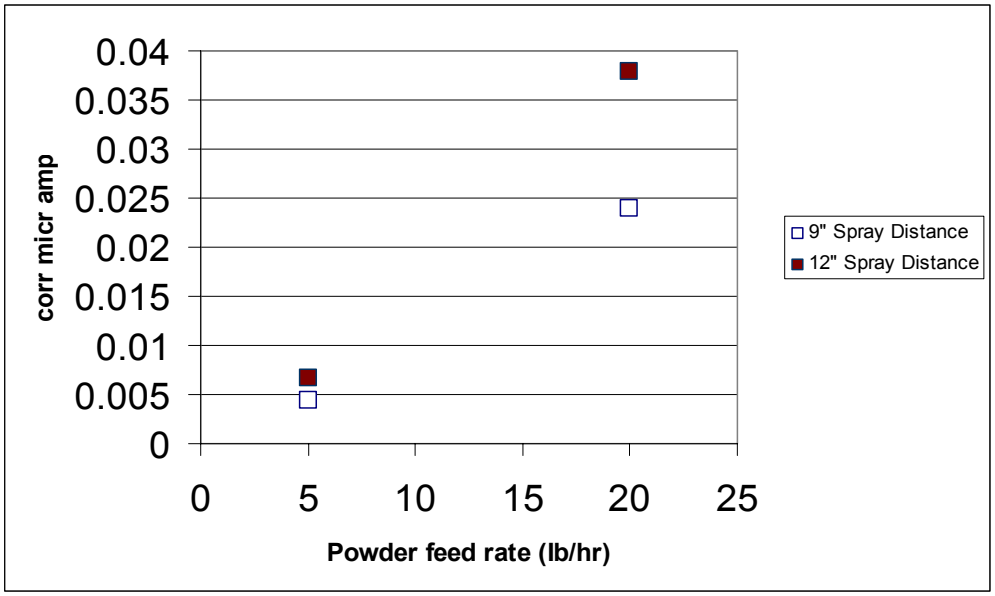

Figure 4.26 I_{Corr} for the different coatings as well as I_{Corr} for Inconel-625 bulk material.

4.4 EROSION TEST RESULTS

Figures 4.27(a, b) show the surfaces of coating 1 and coating 2 after implementing the jet impingement test (erosion test). Weight loss measurements for all coatings for one day (24 hours) run are shown in table 4.6(a) and for 11 days (264 hours) run are shown in Table 4.6(b). Two samples of each coating condition were tested and the results showed a slight variation in between the samples of similar coating condition. However, the variation in between the coating conditions was clear. These measurements were taken before and after cleaning the tested samples and no significant effect of cleaning on weight measurements was observed.

The final weight loss measurements were taken after cleaning. Figure 4.28 shows that the coating erosion is highly affected by the powder feed rate than spray distance. It was noted also that as both spray distance and powder feed rate increased, coating erosion increased (Figure 4.29).

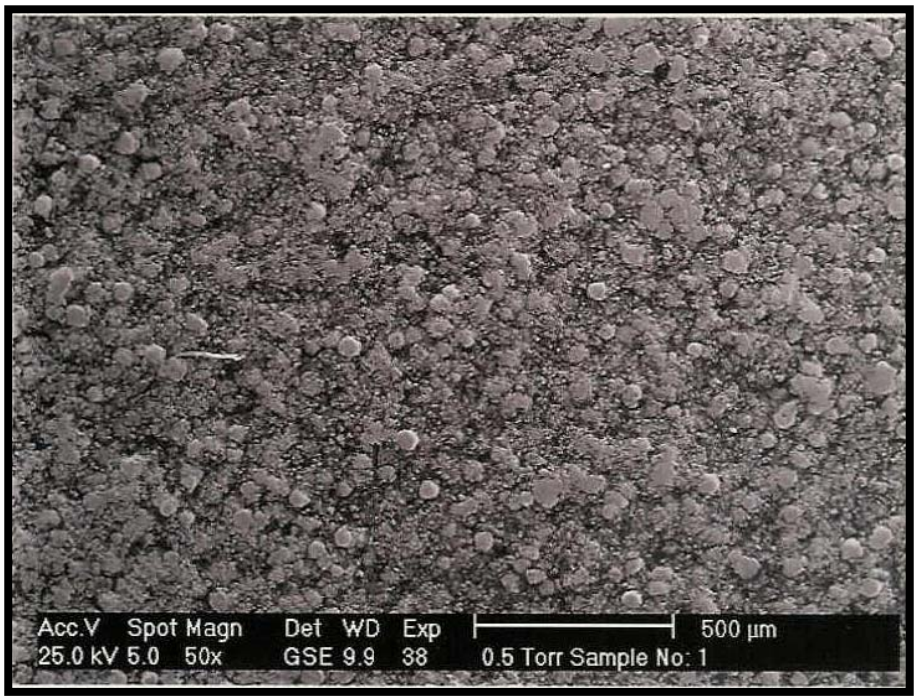

Figure 4.27 (a) Erosion effect due to flow impingement on coating 1 surface at 50x.

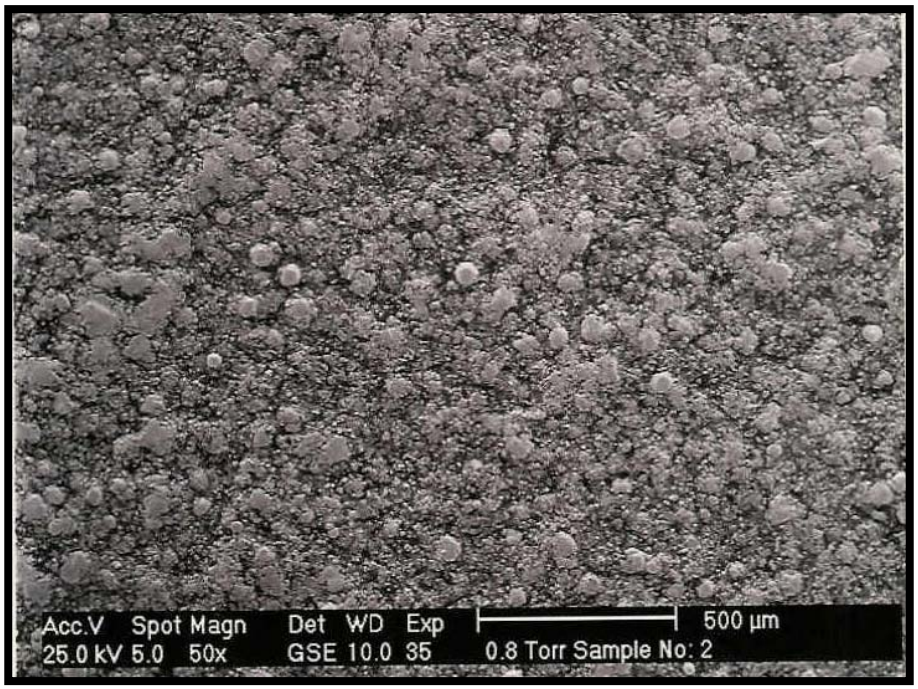

Figure 4.27(b) Erosion effect due to flow impingement on coating 2 surface at 50x

Table 4.6(a). Average weight loss for the four coatings (erosion test) for one day run.

Coating	Initial Wt (g)	Final Wt (Before Cleaning) (g)	Final Wt (After Cleaning) (g)	Wt Loss (g/day)	Avg. Wt Loss (g/day)
1	14.0930	14.0844	14.0787	0.0143	0.0146
	22.8460	22.8360	22.8310	0.015	
2	13.4512	13.4357	13.4312	0.020	0.0275
	13.1994	13.1704	13.1644	0.035	
3	13.5385	13.5295	13.5012	0.0373	0.0401
	13.1995	13.1899	13.1565	0.0429	
4	16.4889	16.4791	16.3989	0.090	0.0943
	13.2127	13.2039	13.1140	0.0987	

Table 4.6(b). Average weight loss for the four coatings (erosion test) for 11 days run.

Coating	Initial Wt (g)	Final Wt (Before Cleaning) (g)	Final Wt (After Cleaning) (g)	Wt Loss (g/day)	Avg. Wt Loss (g/11day)
1	14.0787	14.0135	14.0072	0.0715	0.0822
	22.8310	22.7436	22.7380	0.093	
2	13.4312	13.3058	13.3002	0.131	0.1792
	13.1644	12.9429	12.9369	0.2275	
3	13.5012	13.2089	13.2028	0.2984	0.2991
	13.1565	12.8615	12.8563	0.3002	
4	16.3989	15.6396	15.6339	0.765	0.8017
	13.1140	12.2815	12.2757	0.8383	

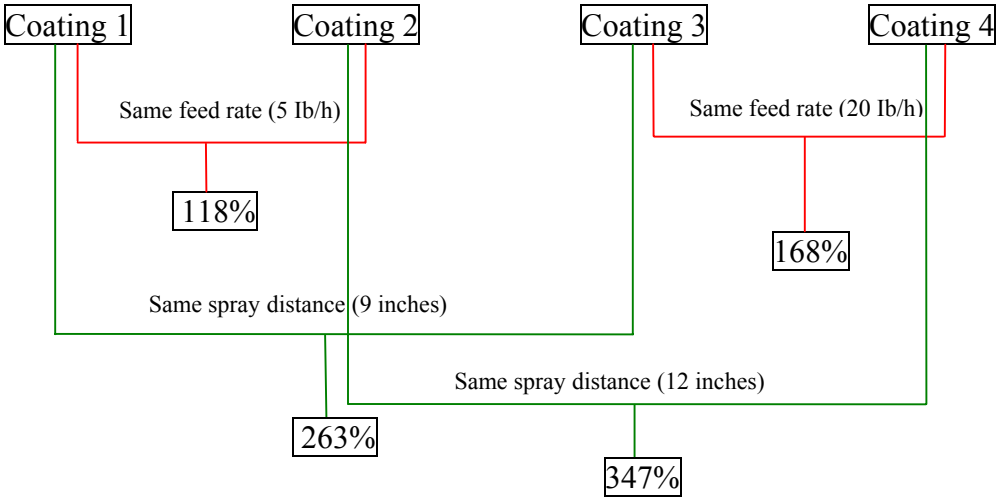

Figure 4.28 Summary of comparison between the spray distance and the powder feed rate effects on coating erosion.

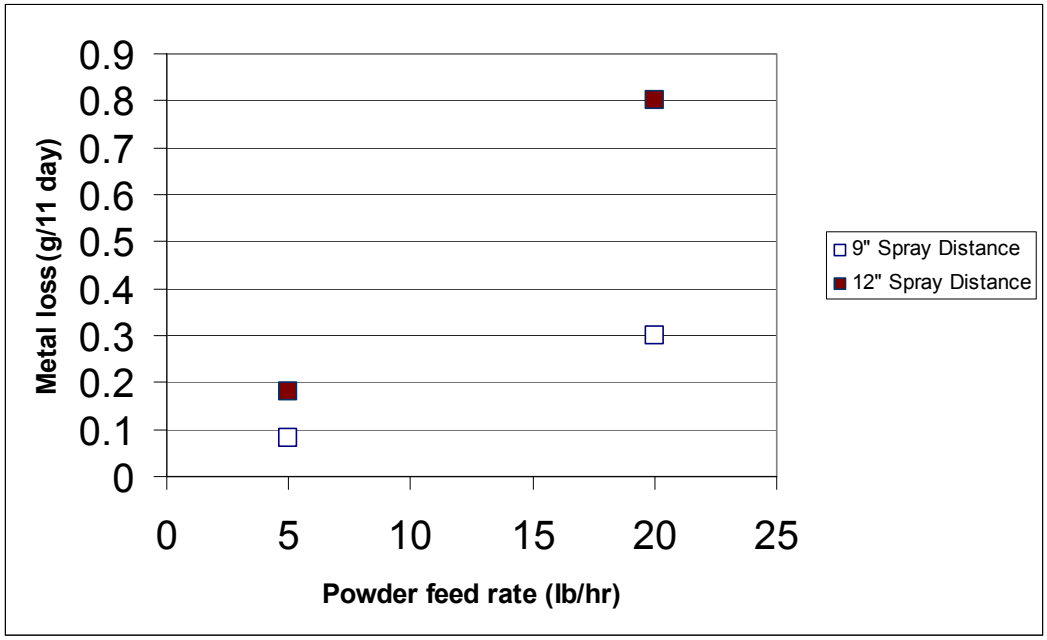

Figure 4.29 Erosion variation with powder feed rate.

4.5 RESULT OF BONDING TEST

The tensile bond strength test was performed using INSTRON 8870 tensile testing machine at a minimum recommended rate of 0.03 in/min. The epoxy used in this test was a German made epoxy (HTR Ultrabond 100) manufactured by HTR Hamburg.GMBH with a tensile strength ,as per manufacturer specification, exceeding 14,000 Psi. To have full curing of the adhesive, the samples were exposed to high temperature 150^{o}C for 80 min as per ASTMC633. Total of 8 samples were tested, two samples from each coating. One sample prematurely failed during testing due to its misalignment.

Due to the non-uniformity of the adhesive distribution in between the coating and the substrate, the test of the first sample failed at 0.035 KN load. This problem was avoided by using another technique to ensure having a uniform distribution in between the coating and the substrate. This technique was to put a tape around the epoxy to hold it during the heating process and to put the sample with the holder in the oven on vertical position rather than horizontal to allow the adhesive to distribute evenly around the coating. Other techniques were used also to enhance bonding in between the coated and the non coated samples during the test. These techniques are:-

a) New Method of Surface Preparation

The first surface preparation was done using fine grit blasting, but since in some of the coated samples, the failure occurs on the epoxy at the surface of the sample and at low load, fine machining of the surface was used instead as another try. In this case also, the epoxy failed before the coating at very small load. The last method of surface preparation was to grind both the coated and the non-coated samples using 60 Grade SiC paper grinder and then clean them twice, first using water and then acetone immediately before putting the adhesive to remove any contamination on the prepared surface.

b) Fabricating New Sample Holder

A new Aluminum sample holder was fabricated with more precise alignment of the two joined samples (Figure 4.30). This holder was fabricated because some of the samples failed during the set up of the machine due to their misalignment. The holder was also modified to allow putting the tape around the adhesive after pressing. In addition, a concentricity check was made for all samples to ensure having minimum misalignment.

Table 4.7. Average fracture strength of the four different coatings.

COATING	AVERAGE FRACTURE STRENGTH (Psi)
Coating 1 (5 Ib/hr 9 inches)	10081
Coating 2 (5 Ib/hr 12 inches)	10302
Coating 3 (20 Ib/hr 9 inches)	7343
Coating 4 (20 Ib/hr 12 inches)	4428

4.5.1 Coating Fracture Strength

Figure 4.31 show a sample of σ-ε curves for each coating. It is shown that coating 1 and 2 with high powder feed rate exhibit high fracture strength than coating 3 and 4 with low powder feed rate. The plot of these curves don't show a straight lines as used to be in the σ-ε curves for solid metals and this is might be due to the microcracks between the coating and the epoxy.

Table 4.7 shows the average of two fracture strength tests of the four different coatings tested. These data show that the powder feed rate is more influencing parameter on coating bonding than spray distance. As the powder feed rate increased, coating bonding decreased.

4.5.2 Variation of Fracture Strength with Feed Rate and Spray Distance

Figure 4.32 shows the variation of coating fracture strength with powder feed rate and spray distance. It is shown that as powder feed rate increases, fracture strength of the coating decreases. In this case, the spray distance is an affecting parameter at high powder feed rate (20 Ib/hr) rather than at low feed rate (5 Ib/hr).

Figure 4.30 Aluminum sample holder for aligning coated and non-coated specimens.

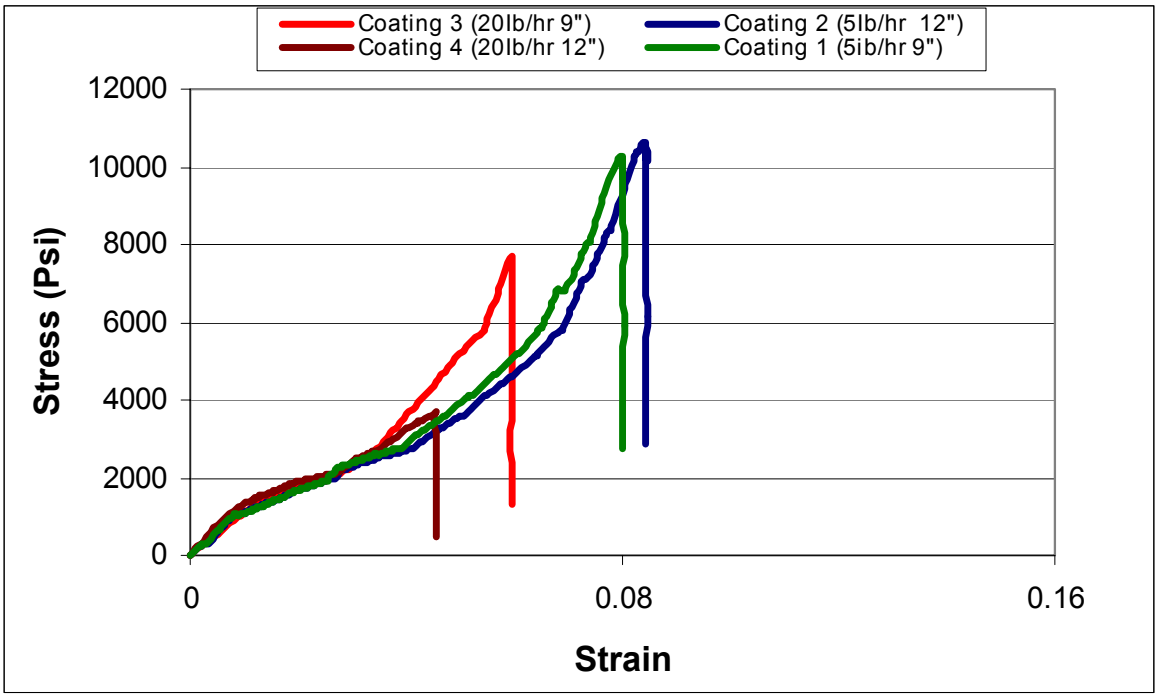

Figure 4.31 Sample σ-ε curves for each coating.

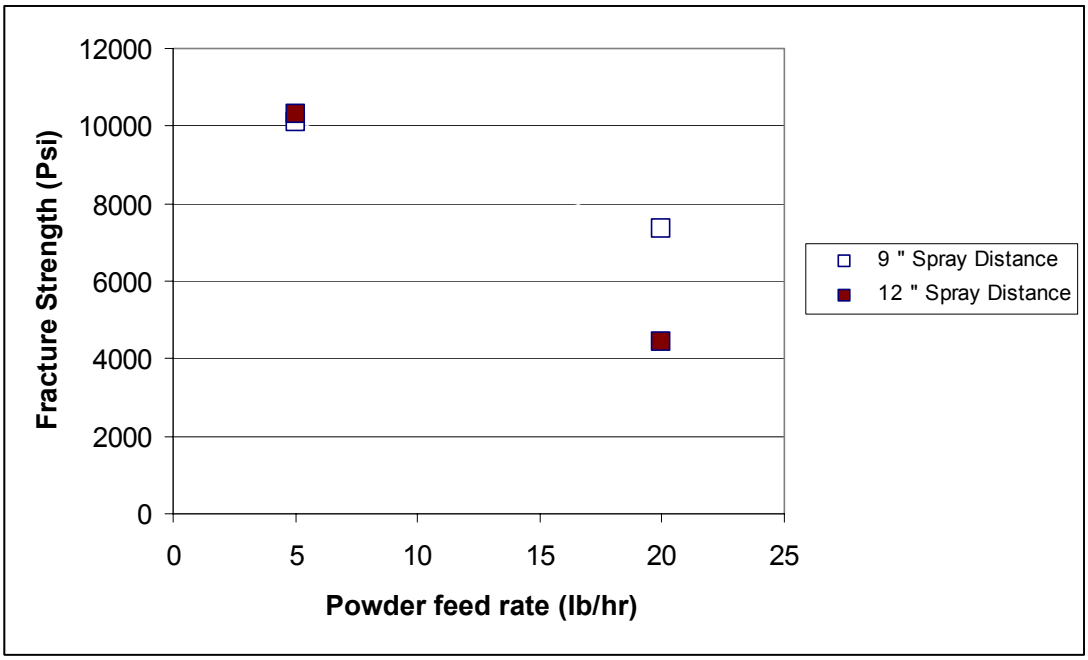

Figure 4.32 Coating fracture strength variation with powder feed rate.

Chapter 5

DISCUSSIONS

5.1 EFFECT OF SPRAY PARAMETERS ON COATING MICROSTUCTURE

Studying the effect of spray parameters such as (powder feed rate and spray distance) on the coating microstructure is vital in determining thermal spray coating quality. By analyzing a cross section of four different coating conditions, it is possible to determine differences between these coatings in terms of porosity and oxide level.

5.1.1 Porosity Variation Due to Powder Feed Rate and Spray Distance

Increasing spray distance produces more porous coating (Figures 4.6). This is probably because at long distances, particles temperature drop which results in low bonding between splats. Regardless of the amount of powder injected to the system, porosity has a proportional relation with the spray distance within specified range. This range for Inconeel-625 powder is 9-12 inches.

Figure 4.6 shows that coating 1 (5 Ib/h feed rate and 9 inches spray distance) is the best in terms of low porosity. However, this level of porosity as per the literature review is the maximum that HVOF coating should produce in comparison with other thermal spray systems (Table 1.1). The reason is that in this study the parameters (spray distance and powder feed rate) considered are the maximum and the minimum values recommended by the manufacturer or something else need to be adjusted or modified in the spraying process. It was expected that the results of the study will reveal the effect of the parameters variation on coating quality and might not be used as optimization for the HVOF coating system unless it considers all other values in between the specified range and many other affecting parameters other than spray distance and powder feed rate.

It was also clear that the powder feed rate has more effect on porosity change than spray distance (Figure 4.6). This is probably because when increasing the powder feed rate from 5 Ib/h to 20 Ib/h at constant energy input, the same amount of energy is used to melt a high amount of material. Hence, one should expect to find non-melted particles within the coating. The presence of non-melted particles increases coating porosity and reduces the bonding between splats. Producing a high amount of porosity up to 5.8 % (Table 4.1), at high powder feed rate is an indication that the powder feeder should be set near to its minimum value.

The results suggest that high quality, HVOF sprayed coatings of low spray distance and low powder feed rate provide significantly better coating quality in terms of low porosity and consequently better coating integrity than the coating produces at high powder feed rate and high spray distance. This work also indicates that there is a relationship between coating

porosity and coating hardness, corrosion and erosion resistance that will be discussed in detail in the following sections.

5.1.2 Oxidation Variation Due to Spray Distance and Powder Feed Rate

EDS x-ray particle analysis for coatings 1-4 reveals that oxygen content in coating 1 and coating 3 with minimum spray distance (9 inches) is lower than coating 2 and coating 4 with maximum spray distance (12 inches), (Figures 4.10-4.13). It is assumed that at longer spray distance with fixed feed rate the oxidation level is higher and this is probably due to the reduction of the momentum of the particles (splats). The reduced momentum increases the traveling time of the particles. This enhances the probability of oxidization of the particles. In other words, the reduction in momentum will allow particles to slow down and oxidize before it hit the substrate surface. The effect of spray distance on coating oxidization is more pronounced than the effect of powder feed rate (Figure 4.14).

Increasing the powder feed rate with fixed spray distances increased the oxide content (Figure 4.15). This is probably due to the reduction in the cooling rate within the coating when the amount of powder injected is high. One should keep in mind that the quantitative measurement of oxygen content is less accurate as compared to heavier elements such as Fe and Ni. Thus, the oxygen measurements are used for comparison purposes rather than absolute values.

5.2 EFFECT OF SPRAY PARAMETERS ON COATING MICRHARDNESS

The Vicker microhardness test is used for all coatings studied. The microhadnness measurements were made on longitudinal and transverse sections. In this work, the microhardness test is used to determine the effect of both spray parameters (spray distance and feed rate) and coating thickness on HVOF coating microhardness.

5.2.1 Microhardness Variation Due to Powder Feed Rate and Spray Distance

Microhardness measurements on both coating cross section and coating surface reveal that coating 1 and coating 2 with low powder feed rate are harder than coating 3 and coating 4. This is might be due to the differences in coating porosity in which the more porous coating has less hardness. Since the increment of the porosity was due to the increment of the spray distance and the powder feed rate, one could think that the best hardness properties could be obtained when the spray distance and the powder feed rate are low. Also, the effect of powder feed rate is more influencing at high spray distance than low spray distance (Figures 4.19-4.20). Results shows that coating porosity is more influencing on coating micrhardness than coating oxidation. This is probably due to the small variation in coatings oxygen content than porosity.

5.2.2 Microhardness Variation with Coating Thickness

Table 4.3 and Figure 4.18 show that a way from the substrate surface, the hardness decreases. However, this reduction is minimal and comes from the weakness of the splats bonding far from the surface. This slight difference in the coating hardness does not significantly affect the overall hardness of the coating. This is primarily due to the uniformity of porosity distribution within the coating.

5.3 INFLUENCE OF SPRAY PARAMETERS ON COATING CORROSION RESISTANCE

Another advantage of using HVOF coating is to reduce corrosion on equipment internal parts. However, this significant feature could be affected by spray parameters variation. This variation in spray parameters such as spray distance and powder feed rate could increase or decrease the coating porosity or oxidization ,as shown before, that may result in variation in the coating corrosion resistance. Although Inconel-625 is recognized as a good corrosion resistance, process parameters variations could significantly affect it. Applications of the HVOF powder are the best suited in seawater where it faces aggressive corrosive environment.

5.3.1 Corrosion Resistance Variation Due to Spray Distance

Table 4.5 shows the I_{Corr} values for all coatings in reference with the bulk material (Inconeel-625 rod). This is mainly aimed to see the difference between the Inconel-625 as a bulk material from that in powder form. The bulk material shows an excellent I_{Corr} value that result from having less porosity and oxidization.

It is clear in this study that porosity and oxide level can significantly affect the coating susceptibility to corrosion. To have better corrosion resistance coating, spray distance has to be short with its specified range (9-12 Inches).

5.3.2 Corrosion Resistance Variation Due to Powder Feed Rate

The results of the I_{Corr} variation with powder feed rate shown in Figure 4.26 reveal that as powder feed rate increased coating corrosion increased. In addition, the effect of the powder feed rate is more pronounced at long spray distance. This is supporting the earlier comments that, the more porous, oxidized coating is the less corrosion resistance.

A possible explanation from the observation that the more porous coating has more susceptibility to corrosion is that, during the operation process of the equipment the electrolyte will penetrate the coating through its porosity and the solution will be stagnant in these voids making a good environment for corrosion. Another important variable that enhances corrosion is the presence of non-melting particles within the coating. These non-melted particles will produce different structures in the coating that will support having enhanced corrosive environment.

Increasing the powder feed rate produce more porous coating with the presence of non-melted particles. This results in reduced corrosion resistance of the HVOF coating.

5.4 INFLUENCE OF SPRAY PARAMETERS ON COATING EROSION RESISTANCE

The reason why this study considered erosion as a wear test among all other types of wear tests is to obtain the results that reflect the practical work of the Inconeel-625 powder in the industrial field. The coated components in the equipments are subjected to high flow impingent of particles contaminated solution. This high flow will impinge the coating surface resulting in surface erosion.

Weight loss measurements for all coatings show that coating 1 is better than coating 2 and coating 3 is better than coating 4 in all cases for the two and the 11days experimental run (Table 4.6 (a,b)). This indicates that variation in the spray distance will affect the coating resistance to erosion regardless of the powder feed rate. Results indicate that as powder feed rate increased coating erosion increased at long spray distance (Figure 4.28). Figure 4.29 shows that the powder feed rate is more affecting parameter in terms of coating erosion than spray distance. This is because as powder feed rate increased, porosity and oxidation increased, microhardness decreased and coating erosion resistance decreased.

5.5 BONDING TEST ANALYSIS OF THE HVOF COATING

As indicated in the ASTM C 633 used in this test, the significance and use of such a test is to control quality and should not be considered to provide an intrinsic value for direct use in making calculations, such as in determining if a coating will withstand specific environmental stress. Because of residual stresses in thermal spray coatings, actual stress depends upon the shape of a particular coated part. Also, in use, a coating may be stressed in a more complex manner than is practical for a standard test.

In this study, coatings with minimum powder feed rate showed high bonding strength. However, coatings with high powder feed rate showed low bonding (Table 4.7). This is probably because as the powder feed rate increased, porosity increased, hardness decreased and tensile bonding decreased. Although there is a clear variation in tensile bonding with respect to spray distance effect at high powder feed rate, this effect is almost negligible at low feed rate and this indicates also that powder feed rate is the most influential parameter (Figure 4.32)

Chapter 6

CONCLUSIONS

The effects of the spray distance and the feeding rate of HVOF coating were studied. Four different coatings were analyzed : i) minimum spray distance with minimum powder feed rate (Coating 1); ii) maximum spray distance with minimum powder feed rate (Coating 2); iii) minimum spray distance with maximum powder feed rate (Coating 3); and iv) maximum spray distance with maximum powder feed rate (Coating 4). Microhardness, corrosion, erosion and bonding tests were used to test these coatings performance. Microstructural investigations for the four coatings conditions were carried out in an attempt to characterize these conditions and determine the coating quality prior to testing.

In light of the results of this study, microstructral investigations reveal that the best coating integrity are obtained with low powder feeding rate and low spray distance within the manufacturer specified range. This combination produced less porosity and less oxide level in the coating. On the other hand, the worst condition of the microstructral study was

obtained when the coating was produced at maximum powder feeding rate and maximum spray distance (Coating 4). Coating 4 exhibited the highest oxide content and porosity within the coating structure.

Microhardness results show that the best coating microstructure has the highest hardness and vise versa. This is probably due to low porosity in the coating. Hardness test results obtained from coating cross section is compatible with the hardness test results obtained from the coating surface.

Corrosion studies also revealed that the coating with low porosity and low oxide content was the coating that had lower I_{Corr}. Comparison of the Inconeel-625 powder and Inconel-625 solid bar reveals the existence of slight difference in corrosion resistance for the best coating integrity (Coating 1) and larg difference for the worst coating integrity (Coating 4). Moreover, the spray distance parameter showed greater influence on I_{Corr} than the powder feeding rate. This is closely related to increased oxide content.

The four coatings conditions are also compared using erosion test. The results show that the resistance of erosion decreased with increased in oxide content and porosity level. Although, there was some difference between the four coating conditions during the first 24 hours erosion test, HVOF coating of all samples showed an excellent resistance to erosion.

Tensile bonding studies also revealed that, the powder feed rate is the mostly affecting parameter on coating bonding. Also, the effect of spray distance is more at high powder feed rate. HVOF coating with minimum powder feed rate has a fracture strength of more than 10,000 Psi which is an excellent adhesion for thermal spray coating.

The present study of HVOF sprayed Inconel-625 coating has demonstrated that spraying process variables are important factors where corrosion and erosion are concerned. Low porosity and oxide content generated from low powder feeding rate and short spray distance within the specified range from the equipment manufacturer, produce hard coating surface with good corrosion and erosion resistance. These coatings are also applicable for the severe corrosion and erosion environments of different industrial applications.

Chapter 6

RECOMMENDATIONS

Mechanical Services Shops Department at Saudi Aramco (MSSD) is implementing the thermal spray as a repair facility since 1986 utilizing plasma spray and since 1990 utilizing HVOF. More than 400 jobs on yearly basis are performed by MSSD saving the company around ($ 3,000,000/year) which makes studying such case important. Because of that, the following recommendations could be highlighted to (MSSD).

- Avoid setting the HVOF powder feeder at its maximum flow rate (20 Ib/h) or near to that. This will produce more porous and oxidized coating. 5 to 12 Ib/h is recommended.
- Adjust the spray distance of the gun to be between 9-10 Inches. This will produce the best coating quality, less porosity, less oxidization, more corrosion and erosion resistance. If the spray distance is too long, the temperature of the particle will drop and the coating becomes more porous. Too short spray distance makes the control of the substrate surface temperature more difficult.
- Utilize proper solvents to remove the aluminum oxide accumulated over the substrate that is caused by the grit blasting material. This will enhance forming a

corrosion layer between the coating and the substrate. Some economical study for this case might be needed.

- Carry out a technology item with King Fahd University of Petroleum and Minerals (KFUPM) to expand the utilization of the HVOF coating process in many different functions in the repair area than limiting the utilization for shaft coatings only. Conducting such a study will save Saudi Aramco a lot of money.

REFERENCES

1. Arsenault.B, Legoux,J.G., Hawthorne.H,.Immarigeon.J.P, Gougeon.P& Moreau. C, "HVOF Process Optimization for the Erosion Resistance of WC-12Co and WC-10Co-4Cr Coatings", in Thermal Spray 2001: New Surfaces for a New Millennium, Singapore, ,Proceedings of the ITSC 2001 Thermal Spray Conference, pp.1051-1060 (2001).

2. Berget. J., "Influence of Powder and Spray Parameters on Erosion and Corrosion Properties of HVOF Sprayed WC-Co-Cr coatings", Norwegian University of Science and Technology, Norway, Engineering Material Science, p. 90 (1998).

3. Bernecki, T., "Coatings for Aggressive Environments," work shop by Northwestern University Basic Industries Research Laboratories, Indianapolis, Proceedings of the ASM material congress, p. 205 (1989).

4. Bezkowiak, J., Fischer, J., and Schwier, G., "Cermets for HVOF processes", HCST Specialist for Specialist, p. 305 (1996).

5. Brandt, O., "The Influence of HVOF Parameters on Microstructure and Wear Resistance of Typical WC-Coating", Proceedings of 17th International SAMPE Europe Conference by ASM International, p. 391-401 (1996).

6. Dorfman, M. R., DeBarro, J. A., "Development and Applications of Corrosion Resistant Thermal Spray Coatings", Proceedings of the 14th International Thermal Spray Conference, p. 567 (1995).

7. Gourlaouen, G., "Influence of Spray Parameters on Stainless Steel Coatings Properties", Proceeding of the 15th ITSC in Nice, France, p. 537-545 (1998).

8. Hackette, C., "The Gas Dynamic of High Velocity Oxygen Fuel Thermal Sprays", ASM International, proceeding of the 13th ITSC in Pennsylvania, USA, p. 315 (1996).

9. Harvey, D., “The Ultimate Coating – Thermal Spraying at Abington.” TWI, Bulletin, p. 456 (1994).

10. Jarosinksi, W. J., Gruninger, M. F., and Londry, C., Characterization of Tungsten Carbide Cobalt Powders and HVOF Coatings, Proceeding of the 1993 National Thermal Spray Conference, p. 153 (1993).

11. Kenneth, K., “Coating and Surface Process”, CRC Inc., New York, Friction Wear Lubrication, p. 232-239 (1996).

12. Kraak, T., Herlaar, W., Wolke, J., De Groot, K., Hydik, E. Al., “Influence of different gases of the mechanical and physical properties on HVOF sprayed tungsten carbide cobalt”, ASM International, Thermal Spray International advances in coatings technology, p. 153-158 (1992).

13. Krepski, R., Nace Staff, “Recent Advances In Spray System Technology”, *Thermal Spray Coating Applications in the Chemical Process Industries*, NACE Intl. for MTI p. 63-69 (1993).

14. Legoux, J.G., Arsenault, B, Moreau.C, Bouyer.V & Leblanc,L. "Evaluation of Four High-Velocity Thermal Spray Guns Using WC-10Co-4Cr Cermets", in Thermal Spray: surface Engineering via Applied Research, Proceedings of the ITSC 2000 Thermal Spray Conference, Montreal, Canada, p.479-486 (2000).

15. Mathami, A., “A study of corrosion control of mild steel using inhibitors under atmospheric conditions”, M.S Thesis, KFUPM, Saudi Arabia, p. 27-29 (2001).

16. Moskowitz, L. N., “Application of HVOF Thermal Spraying to Solve Corrosion Problems in the Petroleum Industry”, Proceedings of the International Thermal Spray Conference, Orlando, Florida, USA, p. 611 (1992).

17. Neiser, R. A., Smith, M. F., Dykhuizen, R. C., “Oxidation in wire HVOF-sprayed steel”, *Thermal Spray Technology*, Vol. 7(4), p. 537-545 (1998).

18. Novinski, E., “Third Global Symposium on HVOF Coatings”, University of Tulsa, San Francisco, CA (1997).

19. Oberkampf, W. L., and Talpallikar, M., "Analysis of a high-Velocity Oxygen-Fuel Thermal Spray Torch: part 2: computational results", *Thermal Spray Technology*, Volume 5(1), p. 62-68. (1996).

20. Parker, D., and Gkutner, "HVOF Spray Technology – Poised for Growth, Advanced Materials and Processes", *Advanced Materials and Processes*, V 4 (9), p. l 68. (1991).

21. Pejryd, L., Wigren J., Gougeon P., and Moreau, C., "Effect of in-flight particle characteristics on the properties of plasma sprayed NiCrALY", Proceedings of the 15th, ITSC, Nice, France, p. 785-790. (1998).

22. Radmard, R., Lachine, C. S., and L. Russo, "Investigation of HVOF Carbides as D-Gun Coating Replacements in the Gas Turbine Industry", Proceedings of the United Thermal Spray Conference, Düsseldorf, Germany, p. 434. (1999).

23. Rao, K., Somerville, D. A, and Lee, D. A, "Properties and Characterization of Coating Made Using Jet Kote Thermal Spray Technique in", Proceeding of the 11th international thermal spray conference, Montreal, Canada: Welding Institute of Canada, p. 873-882. (1986).

24. Rogne, T., Solem, T., and Berget, J., "Effect of Composition and Corrosion Properties of the Metallic Matrix on the Erosion Corrosion Behavior of HVOF Sprayed WC-Coatings.", *Thermal Spray Technology*, p. 495. (1996).

25. Sasaki, M., Kawakami, F., Kmaki, E., and Ishida, M., "Characterization of HVOF Sprayed Cr_3C_2 Coatings", Proceedings of the International Thermal Spray Conference and Exposition, Orlando, Florida, USA, , p. 165. (1992).

26. Schwetzke, R., and Kreye, H., "Microstructure and Properties of Tungsten Carbide Coatings Sprayed with various HVOF Spray Systems" Proceedings of the 15th International Thermal Spray Conference", Nice France, p. 187. (1998).

27. Shimiz Y., Sugiura, K., "An Attempt to Improve the Deposition Efficiency of (Al_3O_3) Coating by HVOF Spraying", Proceeding of the 1st International Thermal Spray Conference on Surface Engineering Via Applied Research, Pub ASM International, Material Park, OH, USA, p. 181-186 (2000).

28. Skandan, G., "Influence of Powder Feed Structure on Wear Properties of HVOF Sprayed WC/Co Hard Coating". Proceeding of the 1st International Thermal Spray Conference On Surface Engineering Via Applied Research, Pub ASM International, Material Park, OH, USA, p. 971-976 (2000).

29. Smith, E., Power, G. D., Barber, T. J., and Chiappeatta, L. M., "Application of Computational Fluid Dynamics on the HVOF Thermal Spray Gun" Proceedings of the 12th ITSC, Orlando, USA, p. 805-810. (1992).

30. Suman, S., "Corrosion and Erosion-Corrosion of High Velocity Oxy-Fuel (HVOF) Sprayed Coatings", Ph.D. Thesis, University of Glasgow, p.236-240. (2000).

31. Swank, W. D., Fincke, J. R., and Haggard, D. C., "HVOF Gas Flow Field Characteristics", Proceedings of the 7th National Thermal Spray Conference, Boston, USA, p. 313-318. (1994).

32. Tucker, R, "Thermal Spray Coating", ASM Handbook Vol. 5. Noyes Pub, 2nd Ed., p. 497-509 (1994).

APPENDIX A

SYSTEM SPRAYING PARAMETERS USING DJ9W SPRAYING GUN (SULZERMETCO 200)

Coating Material (Diamalloy)	PRESSURE			FLOWMETER READING			FLOW-1			POWDER FEEDER			SPRAY PARAMETERS	
	OXYGEN PRESS. (bar)	FUEL PRESS. (bar)	AIR PRESS. (bar)	OXYGEN F.M.R.	FUEL F.M.R.	AIR F.M.R	OXYGEN FLOW NLPM	FUEL FLOW NLPM	AIR FLOW NLPM	N2 F.M.R.	N2 FLOW NLPM	AIR VIB bar	SPR. RATE (Ib/hr.)	SPR. DIST. (Inch)
1003	10.3	6.2	7.2	24	40	50	152	72	399	55	12.5	1.4	5-20	9-12
1004	10.3	6.2	7.2	24	40	50	152	72	399	55	12.5	1.4	5-20	9-12
1005	10.3	6.2	7.2	24	40	50	152	72	399	55	12.5	1.4	5-20	9-12
1006	10.3	6.2	7.2	24	40	50	152	72	399	55	12.5	1.4	5-20	9-12
1007	10.3	6.2	7.2	24	40	50	152	72	399	55	12.5	1.4	5-20	9-12
1008	10.3	6.2	7.2	24	40	50	152	72	399	55	12.5	1.4	5-20	9-12
2003	10.3	6.2	7.2	24	40	50	152	72	399	55	12.5	1.4	5-15	7-10
2004	10.3	6.2	7.2	24	40	50	152	72	399	55	12.5	1.4	5-15	7-10
2005	10.3	6.2	7.2	24	40	50	152	72	399	55	12.5	1.4	5-15	7-10
2006	10.3	6.2	7.2	24	40	50	152	72	399	55	12.5	1.4	5-15	7-10
3001	10.3	6.2	7.2	24	40	50	152	72	399	55	12.5	1.4	5-15	7-10
3002	10.3	6.2	7.2	24	40	50	152	72	399	55	12.5	1.4	5-15	7-10
3004	10.3	6.2	7.2	24	40	50	152	72	399	55	12.5	1.4	5-15	7-10
3005	10.3	6.2	7.2	24	40	50	152	72	399	55	12.5	1.4	5-15	7-10
3006	10.3	6.2	7.2	24	40	50	152	72	399	55	12.5	1.4	5-15	7-10
3007	10.3	6.2	7.2	24	40	50	152	72	399	55	12.5	1.4	5-15	7-10
4006	10.3	6.2	7.2	24	40	50	152	72	399	55	12.5	1.4	5-15	7-10
4008	10.3	6.2	7.2	24	40	50	152	72	399	55	12.5	1.4	5-20	7-10

APPENDIX B

HYBRID COOLED SPRAYING GUN SPECIFICATIONS, [SULZERMECTO, 2000]

VARIABLE	Hybrid Cooling	
	S.I. Units	U.S. Units
Gas Velocity	2140 m/s	7000 ft/s
Combustion pressure	6.9 bar	100 psig
Total heat output	113 kw	385,000 BTU/h
Heat loss to water (cooling capacity)	8.8 kw	30,000 BTU/h
Maximum inlet water temperature	23.9 C	75 F
Minimum water flow	9.51/min	2.5 US gal/min
Water Quality	Drinking water quality or better	
Maximum Spray rate	150 g/min	20 lb/h
Oxygen (O2) pressure	12 bar	170 psig
Oxygen flow	307 NLPM	700 SCFH
Air pressure	7.2 bar	105 psig
Air flow	439 NLPM	1000 SCFH
NITROGEN (N2) carrier pressure	12.1 bar	175 psig
Nitrogen carrier flow	18 NLPM	40 SCFH
Propane (C3 H8)Pressure	6.2 bar	90 psig
WEIGHT-DJM gun body	1.24 kg	2.7 lb
Weight – DJ8H OR DJ9H gun body	1.70 kg	3.7lb
Weight-gun handle	0.23 kg	0.5
Weight – front gun section	2.17 kg	4.8lb

VITA

Author: Hussain Yahya Essa Al Fadhli

- Joined KFUPM after graduation from High School in 1992.
- Graduate from KFUPM as a Mechanical Engineer in June 1997.
- Joined Saudi Aramco on December 1997 and still working in the Mechanical Services Shops Department (MSSD) as a Metallurgical Engineer.
- Started as a part-time Master student at KFUPM in 1999.
- Graduated with a Master Degree in Science of Mechanical Engineering from KFUPM in June 2003.